Journal of Medicinal Chemistry

Article

Cite This: J. Med. Chem. 2019, 62, 6630−6644

pubs.acs.org/jmc

Route to Prolonged Residence Time at the Histamine H_1 Receptor: Growing from Desloratadine to Rupatadine

Reggie Bosma,[†,⊥] Zhiyong Wang,[†,⊥] Albert J. Kooistra,[†,#] Nick Bushby,[§] Sebastiaan Kuhne,[†] Jelle van den Bor,[†] Michael J. Waring,[∥,▽] Chris de Graaf,[†,○] Iwan J. de Esch,[†] Henry F. Vischer,[†] Robert J. Sheppard,[‡] Maikel Wijtmans,[†] and Rob Leurs*[,†]

[†]Amsterdam Institute for Molecules, Medicines and Systems, Division of Medicinal Chemistry, Faculty of Science, VU University Amsterdam, De Boelelaan 1083, 1081 HV Amsterdam, The Netherlands

[‡]Medicinal Chemistry, Research and Early Development, Cardiovascular, Renal and Metabolism, BioPharmaceuticals R&D, AstraZeneca, Gothenburg 431 50, Sweden

[§]Operations, BioPharmaceuticals R&D, AstraZeneca, Alderley Park, Macclesfield SK10 4TG, United Kingdom

[∥]Medicinal Chemistry, Research and Early Development, Oncology R&D, AstraZeneca, Alderley Park, Macclesfield SK10 4TG, United Kingdom

Supporting Information

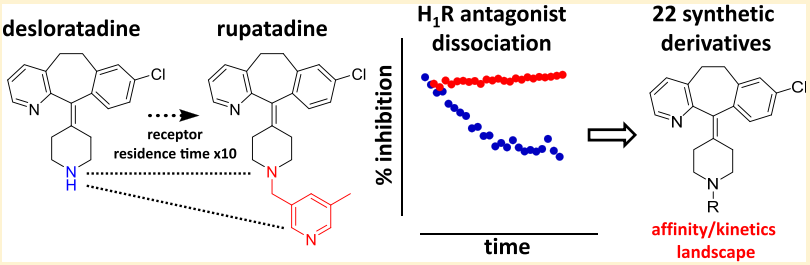

ABSTRACT: Drug−target binding kinetics are an important predictor of in vivo drug efficacy, yet the relationship between ligand structures and their binding kinetics is often poorly understood. We show that both rupatadine (**1**) and desloratadine (**2**) have a long residence time at the histamine H_1 receptor (H_1R). Through development of a [^{3}H]levocetirizine radiolabel, we find that the residence time of **1** exceeds that of **2** more than 10-fold. This was further explored with 22 synthesized rupatadine and desloratadine analogues. Methylene-linked cycloaliphatic or β-branched substitutions of desloratadine increase the residence time at the H_1R, conveying a longer duration of receptor antagonism. However, cycloaliphatic substituents directly attached to the piperidine amine (i.e., lacking the spacer) have decreased binding affinity and residence time compared to their methylene-linked structural analogues. Guided by docking studies, steric constraints within the binding pocket are hypothesized to explain the observed differences in affinity and binding kinetics between analogues.

INTRODUCTION

Drugs have to bind a therapeutically relevant target to exhibit a biological effect and, as such, target binding is well characterized during the development process of many drugs. The binding affinity is an often-used parameter to measure drug binding to a target (quantified as K_D or K_i values), implicitly assuming ligand binding occurs under equilibrium conditions. However, drug pharmacodynamics can also be characterized by the drug−target binding kinetics, which provide important details about the mechanism of target binding, unexplained by solely the binding affinity.[1−3] The drug−target residence time, which is a measure for the lifetime of a drug−target complex, is currently discussed as one of the important contributors to the biological efficacy of drugs in vivo.[3−10] It has been postulated that a suitably long drug−target residence time might increase the therapeutic window in vivo when clearance of the drug is faster than the dissociation of the drug from the receptor.[11,12] In such cases, drug action would last longer than the presence of free drug plasma concentrations (i.e., hysteresis). Thus, duration of therapeutic action may not only depend on drug absorption, distribution, metabolism, and excretion (and the nature of its metabolites), but can also be a direct effect of prolonged target binding.[13−15]

As the target of 33% of all small-molecule drugs, G protein-coupled receptors (GPCRs) are an important class of proteins in drug discovery.[16] The histamine H_1 receptor (H_1R) is an archetypical GPCR and is successfully targeted by antagonists for the treatment of, for example, allergic disorders.[17] A long duration of action has been observed in vivo for second-generation H_1R antagonists like levocetirizine and fexofenadine, which have a long residence time at the H_1R.[18,19]

Received: March 18, 2019
Published: June 20, 2019

DOI: 10.1021/acs.jmedchem.9b00447
J. Med. Chem. 2019, 62, 6630−6644

Scheme 1. Synthesis of [^{3}H]Levocetirizine[a]

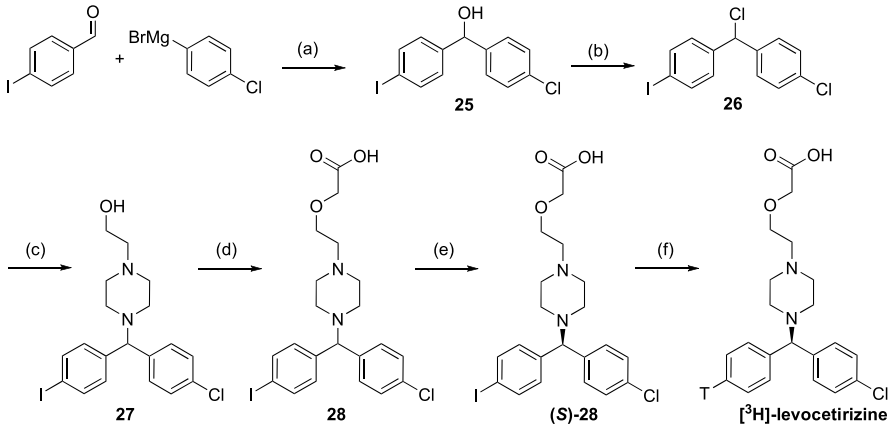

[a]Key: (a) Et_2O, 0 °C to room temperature (rt), 16 h, 88 %; (b) $SOCl_2$, dichloromethane (DCM), rt, 20 h, 95 %; (c) 2-(piperazin-1-yl)ethanol, PhMe, 80 °C, 20 h, 21 %; (d) (1) KOH, dimethylformamide (DMF), 0 °C, 90 min; (2) sodium 2-chloroacetate, DMF, 0 °C, 3 h, 57 %; (e) chiral separation; (f) T_2, Pd/C (10 %), Et_3N, EtOH.

Hysteresis was indeed observed for levocetirizine and fexofenadine.[18−20] A strong hysteresis of H_1R antagonism has also been shown for rupatadine (**1**), which antagonizes the histamine-induced flare response up to 72 h after oral administration, whereas plasma levels could only be detected up to 12 h after administration.[21] This might be explained by the metabolism of rupatadine to metabolites such as desloratadine (**2**), which is a known antihistamine itself with a long H_1R residence time (>1 h) and a long plasma half-life in vivo (human).[19,21−27] Yet, a potentially long drug−target residence time of rupatadine may also be a crucial contributing factor to its observed long duration of action.

Here, we report the measurement of the residence times of rupatadine and desloratadine at the H_1R. It was shown that rupatadine has a ≥10-fold longer residence time at the H_1R, relative to desloratadine. As a consequence, rupatadine completely antagonized the histamine-induced calcium mobilization in HeLa cells for >2 h after removal of unbound antagonist, whereas inspected under the same conditions, desloratadine allowed a time-dependent gradual recovery of the histamine-induced response. To understand the structure−kinetics relationship (SKR) for rupatadine and desloratadine in more detail, the binding kinetics at the H_1R were characterized for newly synthesized analogues (**3**−**24**) that retain the core scaffold of **1** and **2** but contain a diverse set of aromatic and aliphatic N-substituents on the piperidine ring. It was shown that relatively small aliphatic N-substitutions were sufficient for a prolonged H_1R residence time compared to desloratadine, unless this was negated by steric interference in the binding pocket.

RESULTS

Binding Properties of Rupatadine and Desloratadine at the H_1R. Based on the long duration of action of rupatadine in vivo,[21] we hypothesized that it would exhibit a long residence time at the H_1R. Therefore, binding of rupatadine and its structural analogue desloratadine to the human H_1R was investigated, initially using [^{3}H]mepyramine and standardized competition binding experiments.[26] The H_1R binding affinity of desloratadine (pK_i 9.1 ± 0.1) determined in these experiments was consistent with previously reported affinity values (pK_i = 8.8−10[24−26]). Rupatadine (pK_i 8.4 ± 0.1) was shown to have a 5-fold lower binding affinity for the H_1R than desloratadine. To the best of our knowledge, the binding affinity of rupatadine on the human H_1R has not been reported in the literature. Its H_1R activity on guinea pig ileum is known, as well as that for a series of derivatives.[28]

Competitive association experiments were subsequently performed to examine the binding kinetics of rupatadine and desloratadine at the H_1R. Initially, [^{3}H]mepyramine was selected as radioligand and experiments were performed at 25 °C with an 80 min incubation time, in the manner described previously.[26] A clear initial overshoot in [^{3}H]-mepyramine binding was observed for both unlabeled ligands (Figure 2A), which is indicative of the long residence times of the unlabeled ligands relative to [^{3}H]mepyramine.[29,30] However, since the binding curves of rupatadine and desloratadine showed similar overshoot patterns, it was difficult to discern differences in their binding kinetics using the Motulsky−Mahan analysis.[30] Desloratadine was found to have a residence time of 190 ± 40 min (similar to that reported in the literature[25,26]), but for rupatadine, the k_{off} value (and thus the residence time) could not be accurately constrained by the model. To overcome this limitation, it was speculated that the residence times of desloratadine and rupatadine at the H_1R might be better discriminated using a radioligand with a longer residence time, and one more closely matched to desloratadine and rupatadine than mepyramine.[31] With this in mind, levocetirizine was considered a better alternative as it is known to have a 100-fold longer residence time at the H_1R than mepyramine.[25] Radiolabeled levocetirizine has previously been disclosed but without synthetic details for its preparation.[25] The radiolabel was prepared by us using a six-step sequence progressing through intermediates **25**−**28**. Separation of the enantiomers of **28**, followed by Pd-catalyzed dehalotritiation of the corresponding aryl iodide delivered the ligand with a specific activity of 956 GBq mmol^{-1} (Scheme 1 and Supporting Information).

[^{3}H]Levocetirizine was then employed in competitive association experiments to characterize the binding kinetics of rupatadine and desloratadine using an incubation time of 6 h (to ensure a steady state in [^{3}H]levocetirizine binding). In the presence of desloratadine, [^{3}H]levocetirizine binding to the H_1R increased gradually over time, whereas in the presence of

DOI: 10.1021/acs.jmedchem.9b00447
J. Med. Chem. 2019, 62, 6630−6644

rupatadine, a clear initial overshoot in [^{3}H]levocetirizine binding was observed (Figure 2). Based on these curve shapes, it is clear that rupatadine has a longer residence time on the H_1R than desloratadine. Fitting the data to the Motulsky–Mahan model[30] did not result in a precise fit of the k_{off} values, but indicated the k_{off} of desloratadine at the H_1R to be >0.03 min^{-1} (P = 95% in all three experiments) corresponding to a residence time of <33 min. In the case of rupatadine, the k_{off} value at the H_1R is <0.0033 min^{-1} (P = 95% in all three experiments), which corresponds to a residence time of >300 min. Thus, rupatadine has a very long residence time at the H_1R, which is at least 10-fold longer than that observed for desloratadine.

Design and Synthesis of Rupatadine Analogues at the H_1R. To identify the structural features that drive the longer residence time of rupatadine compared to desloratadine at the H_1R, various analogues were synthesized and pharmacologically characterized.

Rupatadine contains a 5-methylpyridin-3-yl group connected through a methylene to the basic amine of desloratadine (Figure 1). To study the SKR, we synthesized analogues with

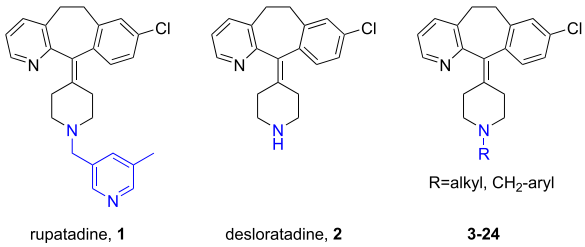

Figure 1. Structures of the investigated H_1R antagonists and synthesized structural analogues.

the methyl group on different positions of the pyridine ring (**3**–**5**), and the pyridine analogue without the methyl group (**6**). Two positional isomers of **6** (**7**, **8**) and two pyrimidines (**9**–**10**) were also prepared. Additionally, the pyridine ring of rupatadine was replaced by a phenyl ring with (**11**), or without (**12**), a 3-methyl group. Finally, to gradually bridge the transition to **2**, a set of analogues was synthesized, in which the basic amine of desloratadine was substituted with a range of alkyl groups (**13**–**24**), varying in size, level of constrainment, and point of attachment (with or without the one-carbon spacer). Of these, only **3**–**8**, **12**, **23**, and **24** have been reported before.[28,32–35]

All rupatidine analogues were efficiently obtained in one step from commercially available desloratidine (**2**), as depicted in Scheme 2. Compounds **4**–**8**, **11**–**12**, and **16** were obtained via nucleophilic substitution of the corresponding alkyl bromides in moderate to good yields (36–86%). Reductive alkylation of **2** with different aromatic aldehydes afforded **3**, **9**, and **10** (64–88% yield). Compounds **13**–**15**, **17**–**20**, **22**, and **23** were synthesized by reductive alkylation using aliphatic carbonyl compounds in acceptable to good yields (52–71%). Methyl derivative **24** was obtained as the fumarate salt from aqueous (aq) formaldehyde and NaBH(OAc)$_3$ in 60% yield. Attempted synthesis of cyclopropyl-substituted analogue **21** via alkylation of **2** with cyclopropylbromide failed. However, reductive alkylation of **2** with (1-ethoxycyclopropoxy)triethylsilane delivered the desired product, albeit in low isolated yield (17%).[36]

Scheme 2. Synthesis of Rupatadine Analogues[a]

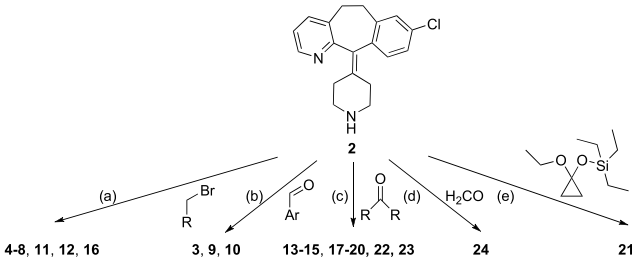

[a]Key: (a) K_2CO_3, DMF, rt, 18 h, 36–86%; (b) NaHB(OAc)$_3$, dichloroethane (DCE), rt, 14 h, 64–88%; (c) NaHB(OAc)$_3$, DCE, rt, 14 h, 52–71%; (d) NaHB(OAc)$_3$, MeOH, DCM, AcOH, rt, 1.5 h, 60% as fumarate salt; (e) NaHB(OAc)$_3$, AcOH, DCM, rt, 48 h, 17%.

Pharmacological Characterization. *H_1R Binding Affinity.* All rupatadine analogues containing an aromatic group (**3**–**12**) had comparable binding affinities at the H_1R (pK_i 7.9–8.5) as rupatadine, which were 4–16-fold lower than the binding affinity of desloratadine (pK_i = 9.1). Substituting the benzene of **12** for a cyclohexane (**13**) did not affect the binding affinity (<2-fold). However, substituting the benzene of **12** for smaller methylene-linked cycloaliphatic N substituents (**14**, **16**, and **17**) resulted in 2–6-fold higher binding affinities at the H_1R, similar to the binding affinity of desloratadine. Likewise, analogues **22**–**24** with small acyclic aliphatic substituents had a high binding affinity at the H_1R as well (pK_i 9.0–9.4), again similar to that of desloratadine (pK_i 9.1). Interestingly, the one-carbon linker between the basic amine and the cyclic aliphatic substituents of **13**, **14**, **16**, and **17** is important for a high-affinity binding, since a 2–8-fold reduced binding affinity is observed for analogues that lack this spacer (**18**–**21**, respectively).

Analysis of Binding Kinetics. To explore the relative residence time of all analogues, a dual-point competition association was performed to determine the kinetic rate index (KRI).[29] This methodology is based on the initial overshoot in radioligand binding when co-incubated with an unlabeled ligand, which is an indicator of a relatively long residence time of the unlabeled ligand compared to that of the radioligand (Figure 2). The overshoot is quantified by measuring the radioligand binding at two time points. The ratio in [^{3}H]levocetirizine binding at both time points (1 and 6 h) is >1 for unlabeled ligands that cause an initial overshoot in [^{3}H]levocetirizine binding and hence have a relatively long residence time compared to [^{3}H]levocetirizine. Using this assay setup, a KRI value of 0.9 ± 0.1 was obtained for unlabeled levocetirizine, demonstrating that, as expected, it has a residence time essentially the same as the radioligand. Desloratadine does not cause an initial overshoot in [^{3}H]-levocetirizine binding (Figure 2B) and has a KRI value of 0.82 ± 0.04. In contrast, rupatadine binds the H_1R with a much longer residence time (Figure 2B), which is indeed reflected by its KRI value of 2.3 ± 0.2 (Table 1). The KRI values for all analogues are given in Table 1. All analogues with an aromatic substituent (**3**–**12**) show KRI values >1, indicative of a consistently long residence time at the H_1R (Table 1). More notably, among the analogues with aliphatic substitutions on the piperidine ring (**1**, **2**, **13**–**24**), large differences in the KRI values were observed (Figure 3). This intriguing SKR in the aliphatic series, in combination with the lack thereof in the aromatic series, led us to focus on the former series.

DOI: 10.1021/acs.jmedchem.9b00447
J. Med. Chem. 2019, 62, 6630–6644

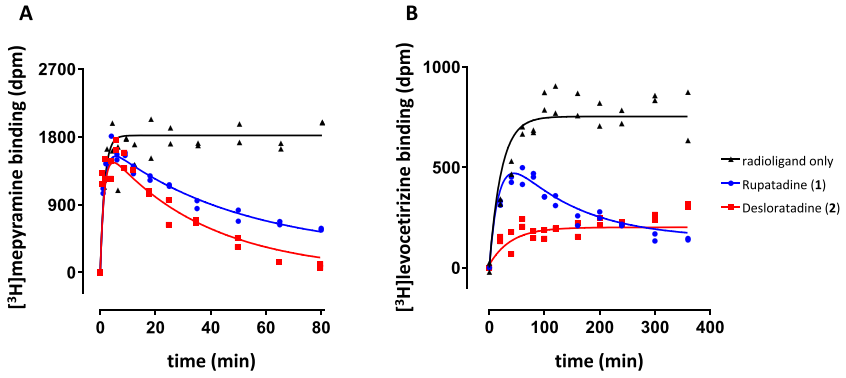

Figure 2. Radioligand association binding when co-incubated with rupatadine and desloratadine. A homogenate of HEK293T cells expressing the H_1R was incubated with: (A) [^{3}H]mepyramine (3.8 nM) alone, or in the presence of either rupatadine (130 nM) or desloratadine (4 nM) or (B) [^{3}H]levocetirizine (6.6 nM) alone, or in the presence of either rupatadine (6 nM) or desloratadine (0.7 nM). Representative graphs of three experiments are shown depicting individual measurements with duplicate values per time point.

Analogues with cycloaliphatic groups and a one-carbon spacer (**13**, **14**, **16**, and **17**) show high KRI values, also indicating a long residence time on the H_1R. However, structural analogues with the same cycloaliphatic group without the one-carbon spacer (**18**–**21**) show similar KRI values to desloratadine, indicative of a shorter residence time at the H_1R. Additionally, analogues with small acyclic aliphatic substituents (**22**–**24**) had an average KRI value slightly larger than 1, implying an increased residence time at the H_1R compared to desloratadine. The correlation between affinity and residence time parameters of GPCR ligands and the physicochemical properties of the ligands has been investigated, including affinities for H_1R receptor antagonists,[37,38] by various research groups.[39−46] Therefore, we investigated whether correlations exist between our pK_i/KRI values and key physicochemical parameters (log $D_{7.4}$, polar surface area, van der Waals volume, pK_a value of the conjugate acid of the piperidine nitrogen atom). However, Figure S1, Tables S1 and S2, show that no strong correlations are evident.

Duration of Functional H_1R Antagonism. Since large differences were observed in the KRI values of the aliphatic rupatadine analogues, these differences were explored in more detail by measuring the kinetics of functional H_1R antagonism following a preincubation with the selected analogues of interest. The functional recovery time (RecT) of the H_1R was previously shown to be correlated with the residence time of antagonists.[47] As such, HeLa cells, with endogenous expression of the H_1R, were preincubated with 10 times the K_i concentration of the respective compound. Unbound ligands were then depleted by washing the cells, which were subsequently stimulated after different incubation times with 10 μM histamine. The intracellular calcium mobilization following administration of histamine was determined with the calcium-sensitive fluorescent dye (Fluo4 NW).

Preincubating HeLa cells with desloratadine, which has a low KRI value (<1), resulted in functional recovery of the H_1R over time (Figure 4A and Table S1). However, cells pretreated with rupatadine were completely unresponsive to histamine, for at least 2 h after removing unbound rupatadine, suggesting very persistent target engagement by rupatadine. In Figure 4B, the functional recovery of the H_1R is compared after pretreating the cells with analogues containing cycloaliphatic N substituents on the piperidine with or without a one-carbon spacer. Analogues with a one-carbon spacer (**14**, **16**, and **17**) completely abolished the histamine-induced calcium response for at least 2 h, similarly to rupatadine. In contrast, and in line with the measured KRI values, removing the one-carbon spacer (**19**–**21**), allowed a relatively fast functional recovery of the histamine response.

The differences in the combined kinetic/affinity binding profiles of the compounds were further explored on a structural level with docking studies. Using the X-ray crystal structure of the H_1R with the structurally related ligand doxepin bound,[48] reference compounds desloratadine, rupatadine, as well as all analogues (**3**–**24**) were docked using PLANTS.[49] Figure 5 shows the postulated binding modes of desloratadine, rupatadine, and the representative pair **14**/**19**, in comparison to the binding mode of the co-crystallized ligand doxepin. Desloratadine likely adopts a similar binding pose to doxepin in the H_1R crystal structure (Figure 5A). Rupatadine was also found to adopt a similar binding mode to doxepin, but its (5-methylpyridin-3-yl)methyl moiety targets an additional area of the H_1R binding pocket toward the extracellular vestibule (Figure 5B). Since the available space in the H_1R pocket next to the amine-binding region is limited by I454$^{7.39}$ and Y458$^{7.43}$, it is postulated that the cyclopentyl substituent of **19** encounters greater steric hindrance than the cyclopentylmethyl substituent of **14** (Figure 5C), in line with the altered H_1R binding characteristics of **19** (Figures 3 and 4B). This steric hindrance results in a tilted binding mode compared to desloratadine, which is not observed for optimal binding of analogues with a methylene spacer between the desloratadine scaffold and the cyclopentyl group (**14**, Figure 5D). The spacer allows the aliphatic group to turn toward the extracellular vestibule (in the direction of H450$^{7.35}$), where more room is available, possibly preventing a steric clash with I454$^{7.39}$ and Y458$^{7.43}$ (Figure 5D).

DISCUSSION AND CONCLUSIONS

A long drug−target residence time has been postulated to benefit the in vivo efficacy of several drugs for a broad number of drug targets, among which is the H_1R.[3,4,7,50,51] Affinity-based optimization of drug binding does not necessarily reflect differences in target residence time,[52,53] and a discrepancy between affinity and residence time at the H_1R was previously described. Moreover, in the case of ligands that do not reach a binding equilibrium within the time frame of a binding experiment, i.e., ligands with a very slow off rate like rupatadine, pK_i will be underestimated.[54] The drug−target residence time can therefore provide additional information for

DOI: 10.1021/acs.jmedchem.9b00447
J. Med. Chem. 2019, 62, 6630−6644

Table 1. H_1R Binding of Rupatadine and Desloratadine Analogues[c]

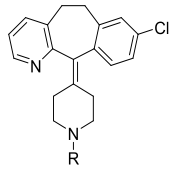

Cmpd#	Name	R	pK_i	KRI
1	rupatadine	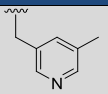	8.4 ± 0.1	2.3 ± 0.2
2	desloratadine	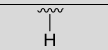	9.1 ± 0.1	0.82 ± 0.04
3[b]	VUF15718	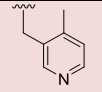	7.89 ± 0.05	2.4 ± 0.4
4[b]	VUF15769	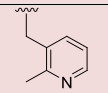	8.05 ± 0.04	5.4 ± 3.5
5[b]	VUF15717	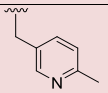	8.12 ± 0.04	5.8 ± 1.7
6[b]	VUF15713	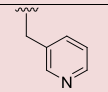	8.3 ± 0.1	4.3 ± 1.5
7[b]	VUF15712	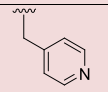	8.1 ± 0.3	3.8 ± 0.5
8[b]	VUF15714	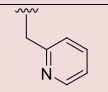	8.5 ± 0.1	2.4 ± 0.5
9	VUF15877	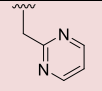	8.5 ± 0.1	1.3 ± 0.1
10	VUF15886	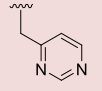	8.3 ± 0.1	1.3 ± 0.1
11	VUF15716	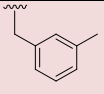	8.1 ± 0.1	3.3 ± 0.9
12[b]	VUF15715	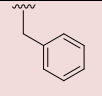	8.4 ± 0.1	1.9 ± 0.5

Cmpd#	Name	R	pK_i	KRI
13	VUF16138	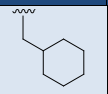	8.6 ± 0.2	1.9 ± 0.3
14	VUF16140	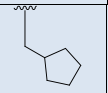	8.9 ± 0.2	1.6 ± 0.2
15	VUF16141	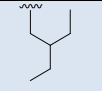	8.75 ± 0.05	1.4 ± 0.2
16	VUF16137	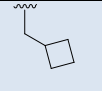	9.1 ± 0.2	1.2 ± 0.1
17	VUF16139	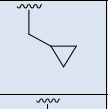	9.2 ± 0.1	1.7 ± 0.1
18	VUF16136	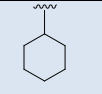	7.7 ± 0.1	0.9 ± 0.1
19	VUF16135	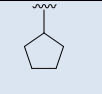	8.4 ± 0.2	0.7 ± 0.1
20	VUF16142	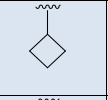	8.67 ± 0.04	0.81 ± 0.04
21	VUF 16219	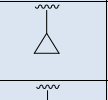	8.5 ± 0.1	0.76 ± 0.03
22	VUF16143	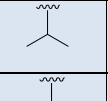	9.0 ± 0.1	1.1 ± 0.3
23[b]	VUF16144	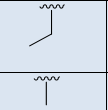	9.38 ± 0.03	1.2 ± 0.1
24[a,b]	VUF15007	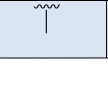	9.4 ± 0.1	1.1 ± 0.2

[a]Fumarate salt. [b]Previously reported (see text for references). [c]Binding affinity (pK_i) values were determined by competition binding experiments using [^{3}H]mepyramine, and KRI values were determined by dual-point competition association experiments using [^{3}H]levocetirizine. Depicted values represent the mean ± standard error of the mean (SEM) of ≥3 experiments

the optimization of drugs that would be lost by focusing on only the binding affinity. Since the residence time is not routinely incorporated in drug development, design strategies for optimizing the drug−target residence time of lead compounds are not widely available. Since rupatadine is shown here to have a much longer residence time at the H_1R than its close structural analogue desloratadine, despite a reduced binding affinity, it provides an opportunity for a detailed investigation of the SKR for this GPCR. Toward this end, we synthesized [^{3}H]levocetirizine, which proved to be a useful tool to map the differences in the KRIs between the two antihistamines. It was therefore employed to determine the

DOI: 10.1021/acs.jmedchem.9b00447
J. Med. Chem. 2019, 62, 6630−6644

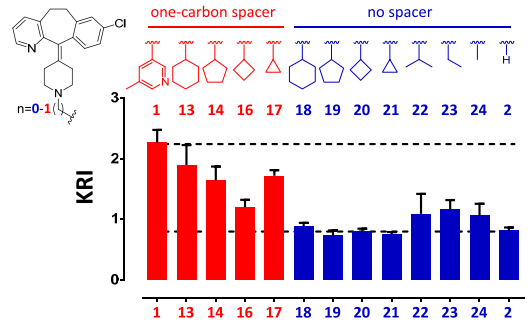

Figure 3. Aliphatic substituents on the basic amine of desloratadine cause differential binding kinetics at the H_1R. A homogenate of HEK293T cells expressing the H_1R was incubated with [^{3}H]-levocetirizine and the respective ligands. Binding of [^{3}H]levocetirizine was determined after 1 and 6 h, and the KRI value was determined as the ratio in [^{3}H]levocetirizine binding at both time points (6/1 h). The bars depict the mean and SEM of ≥3 experiments. The top and bottom dotted lines represent the KRI of reference ligands 1 and 2, respectively.

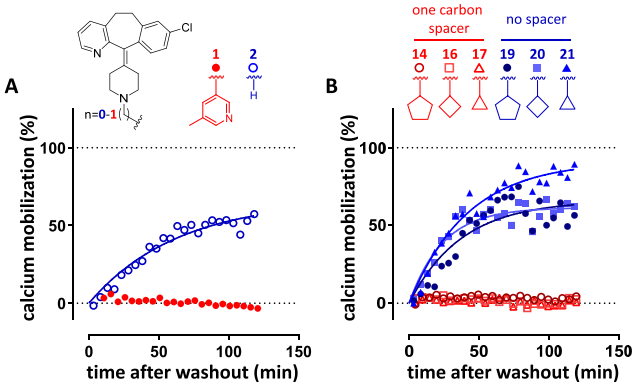

Figure 4. Functional recovery of histamine-induced calcium mobilization after a preincubation with ligands that bind the H_1R. HeLa cells were preincubated for 18−20 h with the respective H_1R ligand, reaching stable and high (±90%) occupancy of the endogenously expressed H_1R. The cells were then labeled with Fluo4 NW in the presence of the respective ligands for 1 h. All excess Fluo4 NW and unbound ligands were removed by wash steps and the cells were subsequently stimulated with histamine (10^{-5} M) after different incubation times. Representative graphs of ≥3 experiments are shown, which depict the normalized calcium mobilization that was measured at each time point after washout. (A) Cells were preincubated with the reference H_1R antagonists: rupatadine (**1**) and desloratadine (**2**). (B) Cells were preincubated with compounds having various cycloalkyl substituents on the basic amine with (**14**, **16**, **17**) or without (**19**, **20**, **21**) a one-carbon spacer.

relative residence times of structural analogues **3**−**24**. Several analogues of rupatadine were designed to replace the (5-methylpyridin-3-yl)methyl group with other aromatic moieties (**3**−**12**). Interestingly, the K_i values of **3**−**12** are within 4-fold of the K_i value of rupatadine. Additionally, all aromatic analogues have a long apparent residence time, as is reflected by the KRI > 1. Removing the aromatic character of the functional group of **12** by replacing it with a cyclohexyl group (**13**) does not affect the observed H_1R binding properties either. Hence, the strong effect on the residence time by the (5-methylpyridin-3-yl)methyl group of rupatadine (compared to desloratadine) cannot be explained by the aromatic character, nor by the pyridine nitrogen atom and the methyl substituent.

To further probe the SKR between rupatadine and desloratadine, a series of analogues were characterized that had different aliphatic substituents on the piperidine group (**13**−**24**). Strikingly, most aliphatic moieties afford an increase in the KRI compared to desloratadine, whereas the binding affinity remains similar or even decreases. For example, **13**−**15** contain relatively large aliphatic substituents (≥6 carbons) and have a slightly reduced binding affinity (pK_i 8.6−8.9) and a high KRI (>1.4) compared to desloratadine. Moreover, analogues with small (≤3 carbons) acyclic aliphatic substituents (**22**−**24**) have a similar binding affinity but still a slightly higher KRI compared to desloratadine. This suggests that growing an aliphatic group from the piperidine increases the residence time at the H_1R. This trend is disrupted, however, for analogues that contain cycloaliphatic groups directly substituted on the amine (**18**−**21**) instead of being separated from the amine by a one-carbon spacer (**13**, **14**, **16**, and **17**). Analogues without the methylene spacer (**18**−**21**) are marked by a diminished KRI and binding affinity compared to analogues with a methylene spacer, whereas the KRI values are of the same magnitude as desloratadine.

This cliff in the SKR trend was validated for a subset of analogues by studying the kinetics of functional H_1R antagonism, which is known to reflect differential residence times at the H_1R.[47] Representative analogues in which the cycloaliphatic group is substituted with a one-carbon spacer (**14**, **16**, and **17**) completely inhibits the functional response of the H_1R for at least 2 h after removal of unbound ligands, as was observed for rupatadine. In contrast, analogues with the same cycloaliphatic groups without a one-carbon spacer (**19**−**21**) allowed a clear recovery of the H_1R functional response, as was also observed for desloratadine. Hence, the relevance of the methylene spacer for the binding kinetics of analogues with relatively large N substituents was confirmed by the duration of functional H_1R inhibition.

The observed residence time/affinity cliff correlated with the binding poses of the representative pair **14** and **19** in the H_1R binding pocket. Our docking studies suggest that the reduced flexibility of the cycloaliphatic group without a spacer (**19**) might lead to a suboptimal fit due to steric hindrance (Figure 5C,D). The increase in ligand residence time at the H_1R, as was observed for most analogues with an aliphatic group on the basic amine of desloratadine (vide supra), seems therefore to be mitigated when the shape of the H_1R binding pocket, i.e., the steric constraints imposed by residues $I454^{7.39}$ and $Y458^{7.43}$, is interfering with the binding position of the desloratadine scaffold.

Recently, it has been shown that N-methylation of H_1R ligands with a primary or secondary amine increased the binding affinity at the H_1R by displacing a water molecule near $I454^{7.39}$.[43] However, this effect on the binding affinity was not observed for analogues with a chlorine moiety on the aromatic rings. Consistent with this finding, N-methylation of desloratadine (which contains a chlorine group), affording **24**, had only modest effects on the H_1R binding affinity. Interestingly, **24** did have a higher KRI compared to desloratadine but not to the same extent as was observed for larger aliphatic substituents (for example, **13**−**17**). Substitution with aliphatic or aromatic groups on the piperidine possibly reduces the resolvation of both the ligand and binding site during a dissociation event. For ligand dissociation from the CRF_1R, for example, a low degree of ligand solvation during egress from the pocket was related to a long residence

DOI: 10.1021/acs.jmedchem.9b00447
J. Med. Chem. 2019, 62, 6630−6644

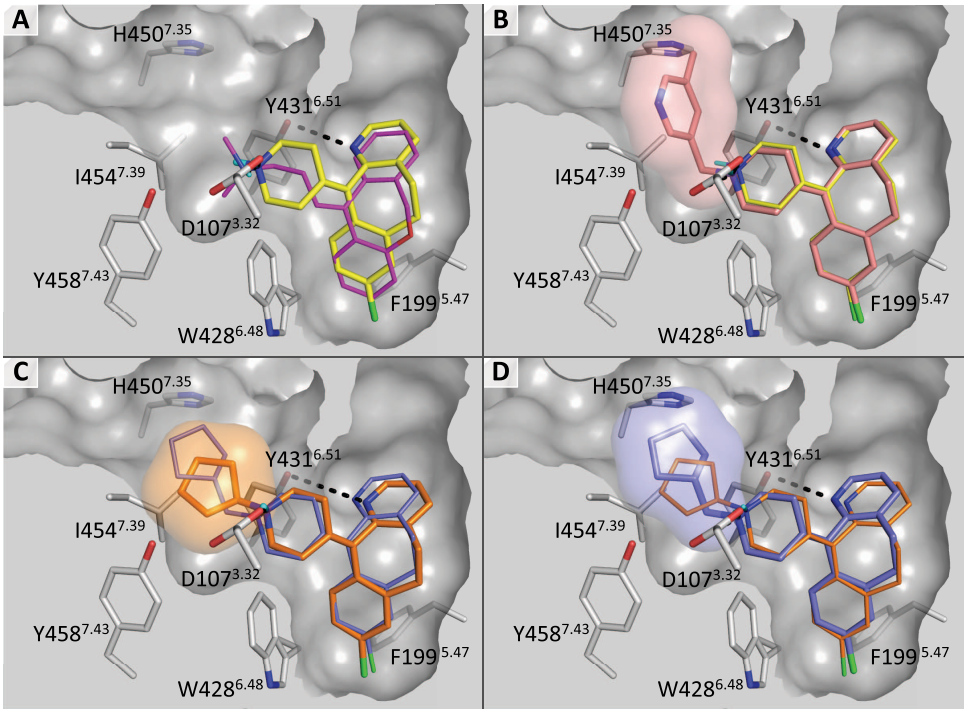

Figure 5. Proposed binding modes of (A) desloratadine (yellow), (B) rupatadine (salmon), and (C, D) compound **19** (orange) in comparison to compound **14** (blue) based on docking[49] into the crystal structure (PDB code 3RZE[48]) of the H_1R in complex with doxepin [magenta; see (A)]. The clipped molecular surface of H_1R highlights the limited space for growing from the amine of desloratadine due to $I454^{7.39}$ and $Y458^{7.43}$. To highlight the fit of the substituents of rupatadine (**2**, B), **19** (C), and **14** (D) compared to desloratadine in the H_1R binding pocket, they are shown as transparent surfaces.

time at the receptor.[41] Moreover, hydrophobic shielding of H bonds can increase the lifetime of such interactions and consequently result in an increased residence time.[40] This is corroborated by the fact that ligands with a relatively high KRI (>1.5) were relatively lipophilic ($\log D_{7.4}$, Figure S1). Considering that N substitution of H_1R ligands was shown to interfere with the water network in the binding site[43] and that the salt bridge between the basic amine of ligands and $D107^{3.32}$ is crucial for a high binding affinity at the receptor,[42] shielding this interaction pair might prevent a rapid egress of the ligands from the binding site.

In conclusion, compared to desloratadine, rupatadine has an extremely long residence time at the H_1R despite an apparent loss in binding affinity, resulting in a longer duration of functional H_1R antagonism. Development of a [^{3}H]-levocetirizine radiolabel allowed a detailed SKR study, which shows that aliphatic N substitution of the piperidine ring from desloratadine is enough to obtain antagonists with a long residence time at the H_1R without increasing the observed binding affinity. Analogues with large flexible cycloaliphatic or aromatic substituents, like the (5-methylpyridin-3-yl)methyl substituent of rupatadine, have a long residence time at the H_1R. Notably, analogues with cycloaliphatic substituents required an additional methylene spacer on the amine for an optimal binding of the H_1R. Modeling studies suggest that the combined affinity/kinetics profiles of analogues without a methylene spacer are possibly linked to the steric complementarity in the ligand–H_1R complex. Aliphatic N substitution of H_1R antagonists is a new potential strategy to optimize the residence time at the receptor. The presented SKR highlights that subtle structural changes of small-molecule ligands can have a profound effect on the binding kinetics at GPCRs.

EXPERIMENTAL SECTION

Pharmacological Assays. All compounds that were tested in pharmacological assays (**1**–**24**, **28**) are confirmed to pass a publicly available pan-assay interference compounds filter.[55,56]

Radioligand Binding Experiments. Radioligand binding experiments were performed as described before, with minor alterations.[26] Cell pellets were produced from HEK293T cells expressing the N-terminally HA-tagged H_1R, and the pellets were stored at −20 °C. Upon experimentation, the cells were thawed, resuspended in radioligand binding buffer [Na_2HPO_4 (50 mM) and KH_2PO_4 (50 mM), pH 7.4], and homogenized with a Branson Sonifier 250 (Branson Ultrasonics, Danbury, CT). Cell homogenates (0.5–3 μg per well) were then incubated with the respective ligands under gentle agitation, as specified for the various assay formats below. After the incubation time, binding reactions were terminated with the cell harvester (PerkinElmer) using rapid filtration and wash steps over polyethyleneimine-coated GF/C filter plates. Filter bound radioligand was then quantified by scintillation counting using MicroScint-O and the Wallac MicroBeta counter (PerkinElmer).

In competition binding experiments, cell homogenates were incubated for 4 h at 25 °C with a single concentration of [^{3}H]mepyramine (1.5–4 nM) and increasing concentrations unlabeled ligands (10^{-5}–10^{-13} M). IC_{50} values were obtained by analyzing the displacement curves with GraphPad Prism 7.03 (GraphPad Software, San Diego) and were converted to K_i values using the Cheng–Prusoff equation.[57]

The binding rate constants of [^{3}H]levocetirizine were determined using the previously described methodology, by using four different concentrations of [^{3}H]levocetirizine (1–35 nM) for a total incubation time of 360 min, with an incubation temperature of 37 °C (data not shown).[26] This resulted in a k_{on} of 3.7 ± 0.4 10^6 min^{-1} M^{-1} and a k_{off} of 0.022 ± 0.003 min^{-1}. In competitive association experiments with [^{3}H]levocetirizine as radioligand, cell homogenates were incubated at 37 °C for various incubation times with a single concentration of [^{3}H]levocetirizine (5–8 nM) in the absence of unlabeled ligand as

DOI: 10.1021/acs.jmedchem.9b00447
J. Med. Chem. 2019, 62, 6630–6644

well as with three different concentrations of either desloratadine (2−60 nM) or rupatadine (0.1−7 nM). The k_{on} and k_{off} values for the binding of [^{3}H]levocetirizine are constrained during the analysis of the H_1R binding kinetics of desloratadine and rupatadine. Kinetic binding rate constants as well as their asymmetrical 95% confidence intervals (95% CI) were determined using GraphPad Prism 7.03. Since the 95% CI values were very broad, the values are depicted to be higher or lower than the 95% CI boundary value observed over all individually performed experiments. Graphs depict a representative graph with mean and standard deviation of duplicate values showing, for clarity, only a single concentration unlabeled ligand.

Competitive association experiments with [^{3}H]mepyramine as radioligand were performed as described before, with minor alterations.[26] Briefly, cell homogenates were incubated at 25 °C for various incubation times with a single concentration of [^{3}H]-mepyramine (2.5−5.5 nM) in the absence or presence of a single concentration unlabeled ligand [desloratadine (4−8 nM) or rupatadine (80−250 nM)].

In dual-point competition association experiments, the kinetic rate index (KRI) value at the H_1R is determined. Cell homogenates were incubated on a 96-well plate for 1 and 6 h at 37 °C, with a single concentration of [^{3}H]levocetirizine (4−11 nM) together with a single concentration of unlabeled ligand that equals the respective K_i value of that ligand at the H_1R. All conditions were measured in triplicate per experiment (n = 3). Additionally, for each 96-well plate, [^{3}H]levocetirizine was incubated with a large excess of mianserin (10^{-5} M) to determine nonspecific binding levels of the radioligand (n = 6) and, as a positive control, [^{3}H]levocetirizine binding was determined in the absence of competitor (maximal binding, n = 6). [^{3}H]levocetirizine binding levels were baseline-corrected by subtracting nonspecific binding levels, and KRI values were then calculated by the ratio of [^{3}H]levocetirizine binding after a 1 h incubation time over the [^{3}H]levocetirizine binding after a 6 h incubation time. KRI is a quantitative measure for the overshoot in radioligand binding, which results from incubating the radioligand with an unlabeled ligand that has a relatively low k_{off}.[29,30] It is therefore crucial that the concentrations of unlabeled ligands are comparable and lead to a submaximal inhibition of the radioligand binding. Therefore KRI values were only accepted when the % inhibition of [^{3}H]levocetirizine binding (compared to the maximal [^{3}H]levocetirizine binding) was (1) less than 80% after either 1 or 6 h and (2) more than 20% inhibition after 6 h. In the case that data points had to be excluded, the concentration unlabeled ligands were attenuated (ranging from 1 × K_i to 3 × K_i concentrations). All experiments were performed in triplicate or more.

Intracellular Calcium Mobilization Assay. The functional recovery of the H_1R following antagonism was measured as described before.[47] In short, HeLa cells, endogenously expressing the H_1R, were seeded 2 × 10^4 cells per well in a clear bottom 96-well plate, which were preincubated overnight with a concentration antagonist corresponding to 10 times the respective K_i at the H_1R (24 wells per antagonist). After 18−20 h, the cells were labeled with the Fluo-4NW dye in the presence of the respective concentration antagonist for an hour. Both the excess dye solution and the unbound antagonists were removed by washing the cells two times, and the cells were then reconstituted in Hank's balanced salt solution buffer supplemented with probenecid (2.5 mM) (t_0). Following the wash step, the cells were stimulated every 5 min by histamine injection, into a single well, using the NOVOstar plate reader (BMG Labtech, Ortenberg, Germany), while simultaneously detecting the calcium-mediated Fluo4 NW fluorescence ($\lambda_{excitation}$ = 494 nm and $\lambda_{emission}$ = 516 nm). For each well stimulated with histamine, a consecutive Triton X-100 injection after 65 s was used to lyse the cells leading to saturation of the Fluo4 NW with calcium. The histamine-induced peak response was then normalized to basal levels of fluorescence (prior to histamine injection; 0) and saturated Fluo4 NW fluorescence (following Triton X-100 injection; 1). This led to a reproducible histamine-induced response over time for HeLa cells pretreated with vehicle condition, which was set to 100%. Histamine-induced peak responses were plotted against the difference in time between t_0 and the subsequent histamine injection. The recovery time (RecT) was determined for antagonists by nonlinear regression using the one-phase association model in GraphPad Prism 7.03.

Molecular Modeling. Simplified molecular-input line-entry system for compounds **1**−**24** were obtained from ChemBioDraw Ultra (version 16.0.1.4) and were subsequently used as input for ChemAxon's calculator for protonation (pH = 7.4). A three-dimensional conformation was then generated using Molecular Networks' CORINA (version 3.49) and stored in Tripos MOL2 format (gold extension). The doxepin-bound H_1R structure was obtained from the protein data bank (PDB code 3RZE), after which the fused T4-lysozyme was removed from the structure. The complex was further prepared for docking using Molecular Operating Environment (Chemical Computing Group, version 2016.0802). Using PLANTS (version 1.2),[49] each compound was docked into the H_1R binding pocket three times with the following settings: search speed, 1; cluster root-mean-square deviation, 1.0; cluster structures, 10; and scored using the ChemPLP scoring function. The binding site was defined by the center of the co-crystallized ligand doxepin with a radius of 11 Å. The resulting docking poses were visually inspected, and the poses with the best overlap with each other as well as the doxepin reference compound were selected, which were also the highest-ranking poses for each compound. Moreover, using an interaction fingerprint similarity analysis,[58] all docking poses were compared to the binding mode of the co-crystallized compound doxepin. All selected docking poses have an interaction fingerprint similarity of at least 0.72 compared to the binding mode of doxepin and are depicted in the Supporting Information (Figures S2 and S3). The binding mode figures were created with PyMol (version 1.8.0).

Chemistry. *General Procedures. Synthesis of Rupatadine Analogues* ***3*****−****24***. Anhydrous tetrahydrofuran, DCM, DMF, and Et_2O were obtained by elution through an activated alumina column prior to use. All other solvents and chemicals were acquired from commercial suppliers and were used as received. ChemBioDraw Ultra 16.0.1.4 was used to generate systematic names for all molecules. All reactions were performed under an inert atmosphere (N_2). Thin-layer chromatography analyses were carried out with alumina silica plates (Merck F_{254}) using staining and/or UV visualization. Column purifications were performed manually using SiliCycle UltraPure silica gel or automatically using Biotage equipment. NMR spectra (^{1}H, ^{13}C, and two-dimensional) were recorded on a Bruker 300 (300 MHz), Bruker 500 (500 MHz), or Bruker 600 (600 MHz) spectrometer. Chemical shifts are reported in parts per million (ppm) (δ), and the residual solvent was used as internal standard (δ ^{1}H NMR: $CDCl_3$ 7.26; dimethyl sulfoxide (DMSO)-d_6 2.50; CD_3OD 3.31; δ ^{13}C NMR: $CDCl_3$ 77.16; DMSO-d_6 39.52; CD_3OD 49.00). Data are reported as follows: chemical shift (integration, multiplicity (s = singlet, d = doublet, t = triplet, q = quartet, br = broad signal, m = multiplet, app = apparent), and coupling constants (Hz)). A Bruker microTOF mass spectrometer using electrospray ionization (ESI) in positive-ion mode was used to record high-resolution mass spectrometry (HRMS) images. A Shimadzu LC-20AD liquid chromatograph pump system linked to a Shimadzu SPD-M20A diode array detector with MS detection using a Shimadzu LC-MS-2010EV mass spectrometer was used to perform liquid chromatography−mass spectrometry (LC−MS) analyses. An Xbridge (C18) 5 μm column (50 mm, 4.6 mm) was used. The solvents that were used were the following: solvent B (acetonitrile with 0.1% formic acid) and solvent A (water with 0.1% formic acid), flow rate of 1.0 mL min^{-1}, start 5% B, linear gradient to 90% B in 4.5 min, then 1.5 min at 90% B, then linear gradient to 5% B in 0.5 min, then 1.5 min at 5% B; and total run time of 8 min. All compounds have a purity of ≥95% (unless specified otherwise), calculated as the percentage peak area of the analyzed compound by UV detection at 254 nm (values are rounded). Reverse-phase column chromatography purifications were performed using Buchi PrepChrom C-700 equipment with a discharge deuterium lamp ranging from 200 to 600 nm to detect compounds using solvent B (acetonitrile with 0.1% formic acid), solvent A (water with 0.1% formic acid), flow rate of 15.0 mL min^{-1}, and a gradient (start 95% A for 3.36 min, then linear gradient to 5% A in 30 min, then at 5% A for

DOI: 10.1021/acs.jmedchem.9b00447
J. Med. Chem. 2019, 62, 6630−6644

3.36 min, then linear gradient to 95% A in 0.5 min, and then 1.5 min at 95% A).

The Supporting Information lists ^{1}H NMR and ^{13}C NMR spectroscopy data as well as high-resolution mass spectroscopy and LC−MS images (Figures S4−S69).

*Synthesis of [^{3}H]Levocetirizine (**25**−**28**).* Column chromatography was carried out using prepacked silica gel cartridges (SiliCycle, Quebec, Canada) on an Isco Companion (Teledyne Isco, NE). ^{1}H NMR spectra were recorded on a Bruker (600 or 400 MHz) using the stated solvent. Chemical shifts (δ) in ppm are quoted relative to $CDCl_3$ (δ 7.26 ppm) and DMSO-d_6 (δ 2.50 ppm). Liquid chromatography−mass spectrometry (LC−MS) data were collected using a Waters Alliance LC (Waters Corporation, MA) with Waters ZQ mass detector. Analytical high-performance liquid chromatography (HPLC) data were recorded using Agilent 1200 HPLC system with a β-Ram Flow Scintillation Analyser, using the following conditions: Waters Sunfire C_{18}, 3.5 μm, 4.6 × 100 mm^2 column at 40 °C, eluting with 5% acetonitrile/water + 0.1% trifluoroacetic acid (TFA) to 95% acetonitrile/water + 0.1% TFA over a 32 min gradient. Specific activities were determined gravimetrically with a Packard Tri-Carb 2100CA Liquid Scintillation Analyser (Packard Instrument Company Inc., IL) using Ultima Gold cocktail. Reactions with tritium gas were carried out on a steel manifold obtained from RC Tritec AG (Teufen, Switzerland). Specific activity was calculated by comparison of the ratio of tritium/hydrogen or carbon-14/carbon-12 for the tracer against the unlabeled reference. [^{3}H]Methyl nosylate was obtained from Quotient Bioresearch as a solution in toluene at 3150 GBq mmol^{-1}. Tritium gas was supplied and absorbed onto a depleted uranium bed by RC Tritec AG (). All other reagents and solvents obtained from Sigma-Aldrich and Fisher and were used without further purification.

*Detailed Experimental Procedures. 8-Chloro-11-(1-((4-methylpyridin-3-yl)methyl)piperidin-4-ylidene)-6,11-dihydro-5H-benzo[5,6]cyclohepta[1,2-b]pyridine (**3**).* A mixture of 4-methylnicotinaldehyde (93 mg, 0.77 mmol), desloratadine (200 mg, 0.643 mmol), and $NaBH(OAc)_3$ (218 mg, 1.027 mmol) in DCE (10 mL) was stirred at room temperature for 12 h. The resulting solution was diluted with water and extracted with DCM. The organic phase was washed with satd. aq $NaHCO_3$ solution. The organic layer was dried over Na_2SO_4, filtered, and concentrated under vacuum. The crude mixture was purified by reverse-phase column chromatography (H_2O/MeCN/HCOOH). The product fraction was evaporated, extracted with DCM/satd. aq Na_2CO_3 solution, dried ($MgSO_4$), and concentrated to yield the title compound as a pink foam (170 mg, 64% yield).

^{1}H NMR (500 MHz, $CDCl_3$) δ 8.42−8.22 (m, 3H), 7.39 (dd, J = 7.6, 1.3 Hz, 1H), 7.15−6.97 (m, 5H), 3.48−3.25 (m, 4H), 2.87−2.60 (m, 4H), 2.51−2.20 (m, 7H), 2.19−2.04 (m, 2H). ^{13}C NMR (126 MHz, $CDCl_3$) δ 157.46, 150.18, 148.22, 147.40, 146.49, 139.49, 138.86, 137.76, 137.35, 133.43, 132.62, 132.56, 132.41, 130.79, 128.94, 125.98, 125.43, 122.13, 57.98, 54.80, 54.71, 31.79, 31.40, 30.97, 30.76, 18.81. HRMS: $C_{26}H_{27}ClN_3$ (M + H)$^+$ calcd: 416.1894, found: 416.1883. LC−MS: t_R = 3.0 min, purity >96% (254 nm), m/z: 416.2 (M + H)$^+$.

*8-Chloro-11-(1-((2-methylpyridin-3-yl)methyl)piperidin-4-ylidene)-6,11-dihydro-5H-benzo[5,6]cyclohepta[1,2-b]pyridine (**4**).* A mixture of desloratadine (155 mg, 0.50 mmol), 3-(chloromethyl)-2-methylpyridine hydrochloride (116 mg, 0.65 mmol), and K_2CO_3 (180 mg, 1.30 mmol) in DMF (10 mL) was stirred at room temperature for 18 h. The mixture was diluted with EtOAc, washed with water (2×) and brine, dried over Na_2SO_4, filtered, and concentrated under vacuum. The crude mixture was purified by reverse-phase column chromatography (H_2O/MeCN/HCOOH) to yield the title compound as a pink foam (120 mg, 58% yield).

^{1}H NMR (500 MHz, $CDCl_3$) δ 8.42−8.31 (m, 2H), 7.59 (d, J = 7.0 Hz, 1H), 7.42 (d, J = 7.6 Hz, 1H), 7.16−7.02 (m, 5H), 3.49−3.29 (m, 4H), 2.88−2.65 (m, 4H), 2.60−2.45 (m, 4H), 2.45−2.26 (m, 3H), 2.23−2.06 (m, 2H). ^{13}C NMR (126 MHz, $CDCl_3$) δ 157.62, 157.44, 147.40, 146.61, 139.50, 138.78, 137.76, 137.32, 137.01, 133.37, 132.69, 132.59, 131.89, 130.78, 128.92, 125.98, 122.11, 121.00, 59.61, 54.92, 54.84, 31.77, 31.41, 30.95, 30.72, 22.26. HRMS: $C_{26}H_{27}ClN_3$ (M + H)$^+$ calcd: 416.1888, found: 416.1906. LC−MS: t_R = 2.9 min, purity >98% (254 nm), m/z: 416.2 (M + H)$^+$.

*8-Chloro-11-(1-((6-methylpyridin-3-yl)methyl)piperidin-4-ylidene)-6,11-dihydro-5H-benzo[5,6]cyclohepta[1,2-b]pyridine (**5**).* A mixture of desloratadine (200 mg, 0.643 mmol), 5-(bromomethyl)-2-methylpyridine hydrobromide (224 mg, 0.836 mmol), and K_2CO_3 (231 mg, 1.67 mmol) in DMF (10 mL) was stirred at room temperature for 18 h. The mixture was diluted with EtOAc, washed with water (2×) and brine, dried over Na_2SO_4, filtered, and concentrated under vacuum. The crude mixture was purified by reverse-phase column chromatography (H_2O/MeCN/HCOOH). The product fraction was evaporated, extracted with DCM/satd. aq Na_2CO_3 solution, dried ($MgSO_4$), and concentrated to yield the title compound as a pink foam (170 mg, 64% yield).

^{1}H NMR (500 MHz, $CDCl_3$) δ 8.41−8.33 (m, 2H), 7.60 (d, J = 7.3 Hz, 1H), 7.41 (d, J = 7.6 Hz, 1H), 7.16−7.02 (m, 5H), 3.50 (s, 2H), 3.42−3.28 (m, 2H), 2.86−2.68 (m, 4H), 2.57−2.48 (m, 4H), 2.47−2.12 (m, 5H). ^{13}C NMR (126 MHz, $CDCl_3$) δ 157.41, 157.37, 149.71, 146.60, 139.51, 138.20, 137.70, 137.42, 137.32, 133.38, 133.00, 132.69, 130.70, 130.1, 128.95, 126.01, 123.01, 122.14, 59.62, 54.56, 54.45, 31.76, 31.42, 30.64, 30.39, 24.10. HRMS: $C_{26}H_{27}ClN_3$ (M + H)$^+$ calcd: 416.1894, found: 416.1886. LC−MS: t_R = 3.0 min, purity >98% (254 nm), m/z: 416.2 (M + H)$^+$.

*8-Chloro-11-(1-(pyridin-3-ylmethyl)piperidin-4-ylidene)-6,11-dihydro-5H-benzo[5,6]cyclohepta[1,2-b]pyridine (**6**).* A mixture of desloratadine (500 mg, 1.61 mmol), 3-(bromomethyl)-pyridine hydrobromide (529 mg, 2.09 mmol), and K_2CO_3 (579 mg, 4.19 mmol) in DMF (10 mL) was stirred at room temperature for 18 h. The mixture was diluted with EtOAc, washed with water (2×) and brine, dried over Na_2SO_4, filtered, and concentrated under vacuum. The crude mixture was purified by reverse-phase column chromatography (H_2O/MeCN/HCOOH) to yield the title compound as a pink foam (430 mg, 66% yield).

^{1}H NMR (500 MHz, $CDCl_3$) δ 8.54−8.43 (m, 2H), 8.37 (d, J = 4.6 Hz, 1H), 7.67 (d, J = 7.7 Hz, 1H), 7.41 (d, J = 7.6 Hz, 1H), 7.25−7.20 (m, 1H), 7.15−7.02 (m, 4H), 3.49 (s, 2H), 3.43−3.27 (m, 2H), 2.88−2.64 (m, 4H), 2.55−2.46 (m, 1H), 2.45−2.25 (m, 3H), 2.21−2.02 (m, 2H). ^{13}C NMR (126 MHz, $CDCl_3$) δ 157.44, 150.40, 148.60, 146.63, 139.51, 138.60, 137.73, 137.34, 136.81, 133.63, 133.40, 132.79, 132.63, 130.81, 128.96, 126.01, 123.37, 122.15, 60.04, 54.73, 54.66, 31.80, 31.42, 30.89, 30.65. HRMS: $C_{25}H_{25}ClN_3$ (M + H)$^+$ calcd: 402.1737, found: 402.1733. LC−MS: t_R = 3.0 min, purity >99% (254 nm), m/z: 402.1 (M + H)$^+$.

*8-Chloro-11-(1-(pyridin-4-ylmethyl)piperidin-4-ylidene)-6,11-dihydro-5H-benzo[5,6]cyclohepta[1,2-b]pyridine (**7**).* A mixture of desloratadine (500 mg, 1.61 mmol), 4-(bromomethyl)-pyridine hydrobromide (529 mg, 2.09 mmol), and K_2CO_3 (579 mg, 4.19 mmol) in DMF (10 mL) was stirred at room temperature for 18 h. The mixture was diluted with EtOAc, washed with water (2×) and brine, dried over Na_2SO_4, filtered, and concentrated under vacuum. The crude mixture was purified by reverse-phase column chromatography (H_2O/MeCN/HCOOH) to yield the title compound as a pink foam (229 mg, 36% yield).

^{1}H NMR (500 MHz, $CDCl_3$) δ 8.49 (d, J = 5.6 Hz, 2H), 8.35 (d, J = 4.6 Hz, 1H), 7.39 (d, J = 7.6 Hz, 1H), 7.24 (d, J = 5.4 Hz, 2H), 7.16−7.00 (m, 4H), 3.46 (s, 2H), 3.42−3.24 (m, 2H), 2.85−2.60 (m, 4H), 2.57−2.23 (m, 4H), 2.20−2.04 (m, 2H). ^{13}C NMR (126 MHz, $CDCl_3$) δ 157.38, 149.64, 147.76, 146.58, 139.50, 138.46, 137.69, 137.38, 133.41, 132.82, 132.63, 130.78, 128.96, 126.00, 123.89, 122.18, 61.56, 54.85, 54.82, 31.77, 31.40, 30.89, 30.67. HRMS: $C_{25}H_{25}ClN_3$ (M + H)$^+$ calcd: 402.1737, found: 402.1741. LC−MS: t_R = 3.0 min, purity >99% (254 nm), m/z: 402.1 (M + H)$^+$.

*8-Chloro-11-(1-(pyridin-2-ylmethyl)piperidin-4-ylidene)-6,11-dihydro-5H-benzo[5,6]cyclohepta[1,2-b]pyridine (**8**).* A mixture of desloratadine (500 mg, 1.61 mmol), 2-(bromomethyl)-pyridine hydrobromide (529 mg, 2.09 mmol), and K_2CO_3 (579 mg, 4.19 mmol) in DMF (10 mL) was stirred at room temperature for 18 h. The mixture was diluted with EtOAc, washed with water (2×) and brine, dried over Na_2SO_4, filtered, and concentrated under vacuum.

DOI: 10.1021/acs.jmedchem.9b00447
J. Med. Chem. 2019, 62, 6630−6644

The crude mixture was purified by reverse-phase column chromatography (H_2O/MeCN/HCOOH) to yield the title compound as a pink foam (399 mg, 62% yield).

^{1}H NMR (500 MHz, $CDCl_3$) δ 8.52 (d, J = 4.5 Hz, 1H), 8.36 (d, J = 4.6 Hz, 1H), 7.62 (t, J = 7.6 Hz, 1H), 7.40 (d, J = 7.2 Hz, 2H), 7.18−6.98 (m, 5H), 3.63 (s, 2H), 3.45−3.27 (m, 2H), 2.87−2.68 (m, 4H), 2.59−2.40 (m, 2H), 2.40−2.27 (m, 2H), 2.26−2.10 (m, 2H). ^{13}C NMR (126 MHz, $CDCl_3$) δ 158.54, 157.56, 149.24, 146.60, 139.52, 138.86, 137.75, 137.28, 136.44, 133.43, 132.62, 132.57, 130.87, 128.96, 125.97, 123.22, 122.11, 122.06, 64.46, 55.07, 55.05, 31.82, 31.40, 30.94, 30.71. HRMS: $C_{25}H_{25}ClN_3$ $(M + H)^+$ calcd: 402.1737, found: 402.1738. LC−MS: t_R = 3.1 min, purity >99% (254 nm), m/z: 402.1 $(M + H)^+$.

*8-Chloro-11-(1-(pyrimidin-2-ylmethyl)piperidin-4-ylidene)-6,11-dihydro-5H-benzo[5,6]cyclohepta[1,2-b]pyridine (**9**).* A mixture of pyrimidine-2-carbaldehyde (91 mg, 0.84 mmol), desloratadine (218 mg, 0.7 mmol), and $NaBH(OAc)_3$ (237 mg, 1.12 mmol) in DCE (10 mL) was stirred at room temperature for 12 h. The resulting solution was diluted with water and extracted with DCM. The organic phase was washed with satd. aq $NaHCO_3$. The organic layer was dried over Na_2SO_4, filtered, and concentrated under vacuum. The crude mixture was purified by column chromatography (EtOAc/MeOH/triethylamine (TEA) = 94:4:2, v/v/v) to yield the title compound as a pink foam (240 mg, 85% yield).

^{1}H NMR (500 MHz, $CDCl_3$) δ 8.71 (d, J = 4.9 Hz, 2H), 8.37 (dd, J = 4.7, 1.4 Hz, 1H), 7.41 (dd, J = 7.7, 1.4 Hz, 1H), 7.17 (t, J = 4.9 Hz, 1H), 7.14−7.02 (m, 4H), 3.86−3.74 (m, 2H), 3.44−3.30 (m, 2H), 2.89−2.71 (m, 4H), 2.65−2.47 (m, 2H), 2.42−2.25 (m, 4H). ^{13}C NMR (126 MHz, $CDCl_3$) δ 167.63, 157.64, 157.20, 146.59, 139.48, 138.78, 137.73, 137.20, 133.43, 132.61, 132.59, 130.89, 128.96, 125.97, 122.07, 119.32, 65.09, 55.25, 55.21, 31.85, 31.40, 30.75, 30.50. HRMS: $C_{24}H_{24}ClN_4$ $(M + H)^+$ calcd: 403.1684, found: 403.1680. LC−MS: t_R = 2.9 min, purity >99% (254 nm), m/z: 403.2 $(M + H)^+$.

*8-Chloro-11-(1-(pyrimidin-4-ylmethyl)piperidin-4-ylidene)-6,11-dihydro-5H-benzo[5,6]cyclohepta[1,2-b]pyridine (**10**).* A mixture of pyrimidine-4-carbaldehyde (91 mg, 0.84 mmol), desloratadine (218 mg, 0.7 mmol), and $NaBH(OAc)_3$ (237 mg, 1.12 mmol) in DCE (10 mL) was stirred at room temperature for 12 h. The resulting solution was diluted with water and extracted with DCM. The organic phase was washed with satd. aq $NaHCO_3$, dried over Na_2SO_4, filtered, and concentrated under vacuum. The crude mixture was purified by column chromatography (EtOAc/MeOH/TEA = 94:4:2, v/v/v) to yield the title compound as a pink foam (248 mg, 88% yield).

^{1}H NMR (500 MHz, $CDCl_3$) δ 9.11 (s, 1H), 8.67 (d, J = 5.2 Hz, 1H), 8.38 (dd, J = 4.7, 1.2 Hz, 1H), 7.53 (d, J = 5.0 Hz, 1H), 7.42 (dd, J = 8.8, 1.2 Hz, 2H), 7.17−7.02 (m, 4H), 3.62 (s, 2H), 3.44−3.31 (m, 2H), 2.87−2.71 (m, 4H), 2.61−2.52 (m, 1H), 2.51−2.42 (m, 1H), 2.41−2.31 (m, 2H), 2.30−2.19 (m, 2H). ^{13}C NMR (126 MHz, $CDCl_3$) δ 167.86, 158.57, 157.38, 157.09, 146.59, 139.52, 138.13, 137.71, 137.37, 133.42, 133.05, 132.71, 130.74, 128.96, 126.03, 122.17, 120.13, 63.36, 55.10, 31.79, 31.44, 30.92, 30.70, one signal overlapping or not visible. HRMS: $C_{24}H_{24}ClN_4$ $(M + H)^+$ calcd: 403.1684, found: 403.1681. LC−MS: t_R = 2.9 min, purity >99% (254 nm), m/z: 403.2 $(M + H)^+$.

*8-Chloro-11-(1-(3-methylbenzyl)piperidin-4-ylidene)-6,11-dihydro-5H-benzo[5,6]cyclohepta[1,2-b]pyridine (**11**).* Desloratadine (500 mg, 1.61 mmol) was added to 3-methylbenzyl bromide (387 mg, 2.09 mmol) and TEA (326 mg, 3.22 mmol) in DCM (10 mL). The resulting mixture was stirred at room temperature for 18 h. The solution was then diluted with DCM, washed with a 5% $NaHCO_3$ solution, then with H_2O, dried over Na_2SO_4, filtered, and concentrated under vacuum. The crude mixture was purified by reverse-phase column chromatography (H_2O/MeCN/HCOOH). The product fraction was evaporated, extracted with DCM/satd. aq Na_2CO_3 solution, dried ($MgSO_4$), and concentrated to yield the title compound as a pink foam (432 mg, 65% yield).

^{1}H NMR (500 MHz, $CDCl_3$) δ 8.39 (dd, J = 4.8, 1.5 Hz, 1H), 7.41 (d, J = 7.7 Hz, 1H), 7.22−6.99 (m, 8H), 3.53−3.28 (m, 4H), 2.90−2.68 (m, 4H), 2.58−2.25 (m, 7H), 2.21−2.04 (m, 2H). ^{13}C NMR (126 MHz, $CDCl_3$) δ 157.69, 146.64, 139.52, 139.18, 138.09, 137.84, 137.78, 137.23, 133.42, 132.57, 132.49, 130.92, 129.97, 128.97, 128.06, 127.79, 126.33, 125.99, 122.08, 62.99, 54.89, 54.85, 31.87, 31.44, 30.99, 30.75, 21.46. HRMS: $C_{27}H_{28}ClN_2$ $(M + H)^+$ calcd: 415.1941, found: 415.1938. LC−MS: t_R = 3.6 min, purity >99% (254 nm), m/z: 415.2 $(M + H)^+$.

*11-(1-Benzylpiperidin-4-ylidene)-8-chloro-6,11-dihydro-5H-benzo[5,6]cyclohepta[1,2-b]pyridine (**12**).* Desloratadine (500 mg, 1.61 mmol) was added to benzyl bromide (358 mg, 2.09 mmol) and TEA (326 mg, 3.22 mmol) in DCM (10 mL). The resulting mixture was stirred at room temperature for 18 h. The solution was then diluted with DCM and H_2O and extraction was performed. The organic layer was dried over Na_2SO_4 and filtered. The crude mixture was purified by reverse-phase column chromatography (H_2O/MeCN/HCOOH). The product fraction was evaporated, extracted with DCM/satd. aq Na_2CO_3 solution, dried ($MgSO_4$), and concentrated to yield the title compound as a pink foam (484 mg, 75% yield).

^{1}H NMR (500 MHz, $CDCl_3$) δ 8.38 (dd, J = 4.8, 1.2 Hz, 1H), 7.42 (dd, J = 7.3, 1.1 Hz, 1H), 7.33−7.20 (m, 5H), 7.17−7.00 (m, 4H), 3.51 (s, 2H), 3.45−3.28 (m, 2H), 2.87−2.69 (m, 4H), 2.58−2.26 (m, 4H), 2.23−2.07 (m, 2H). ^{13}C NMR (126 MHz, $CDCl_3$) δ 157.64, 146.62, 139.51, 139.04, 138.09, 137.81, 137.26, 133.42, 132.58, 132.54, 130.89, 129.23, 128.96, 128.21, 127.06, 125.99, 122.10, 62.91, 54.79, 54.74, 31.85, 31.42, 30.94, 30.71. HRMS: $C_{26}H_{26}ClN_2$ $(M + H)^+$ calcd: 401.1785, found: 401.1779. LC−MS: t_R = 3.4 min, purity >99% (254 nm), m/z: 401.1 $(M + H)^+$.

*8-Chloro-11-(1-(cyclohexylmethyl)piperidin-4-ylidene)-6,11-dihydro-5H-benzo[5,6]cyclohepta[1,2-b]pyridine (**13**).* A mixture of cyclohexanecarbaldehyde (95 mg, 0.84 mmol), desloratadine (218 mg, 0.70 mmol), and $NaBH(OAc)_3$ (238 mg, 1.12 mmol) in DCE (10 mL) was stirred at room temperature for 12 h. The resulting solution was diluted with water and extracted with DCM. The organic phase was washed with satd. aq $NaHCO_3$ solution. The organic layer was dried over Na_2SO_4, filtered, and concentrated under vacuum. The crude mixture was purified by column chromatography (cyclohexane/EtOAc/TEA = 40/58/2, v/v/v) to yield the title compound as a pink foam (180 mg, 63% yield).

^{1}H NMR (500 MHz, $CDCl_3$) δ 8.39 (d, J = 4.6 Hz, 1H), 7.42 (d, J = 7.6 Hz, 1H), 7.16−7.09 (m, 3H), 7.07 (dd, J = 7.7, 4.8 Hz, 1H), 3.46−3.29 (m, 2H), 2.86−2.74 (m, 2H), 2.74−2.63 (m, 2H), 2.55−2.46 (m, 1H), 2.44−2.25 (m, 3H), 2.14−1.97 (m, 4H), 1.80−1.60 (m, 5H), 1.50−1.38 (m, 1H), 1.26−1.07 (m, 3H), 0.91−0.78 (m, 2H). ^{13}C NMR (126 MHz, $CDCl_3$) δ 157.77, 146.74, 139.66, 137.96, 137.35, 133.54, 132.70, 132.55, 130.96, 129.07, 126.10, 122.18, 65.45, 55.51, 55.41, 35.32, 32.16, 32.13, 31.94, 31.55, 30.87, 30.62, 26.82, 26.25, one aromatic signal overlapping or not visible. HRMS: $C_{26}H_{32}ClN_2$ $(M + H)^+$ calcd: 407.2249, found: 407.2231. LC−MS: t_R = 3.6 min, purity >99% (254 nm), m/z: 407.2 $(M + H)^+$.

*8-Chloro-11-(1-(cyclopentylmethyl)piperidin-4-ylidene)-6,11-dihydro-5H-benzo[5,6]cyclohepta[1,2-b]pyridine (**14**).* A mixture of cyclopentanecarbaldehyde (83 mg, 0.84 mmol), desloratadine (218 mg, 0.70 mmol), and $NaBH(OAc)_3$ (238 mg, 1.12 mmol) in DCE (10 mL) was stirred at room temperature for 12 h. The resulting solution was diluted with water and extracted with DCM. The organic phase was washed with satd. aq $NaHCO_3$ solution. The organic layer was dried over Na_2SO_4, filtered, and concentrated under vacuum. The crude mixture was purified by column chromatography (cyclohexane/EtOAc/TEA = 40/58/2, v/v/v) to yield the title compound as a pink foam (162 mg, 59% yield).

^{1}H NMR (500 MHz, $CDCl_3$) δ 8.39 (d, J = 4.6 Hz, 1H), 7.41 (d, J = 7.7 Hz, 1H), 7.15−7.08 (m, 3H), 7.06 (dd, J = 7.6, 4.9 Hz, 1H), 3.45−3.29 (m, 2H), 2.86−2.69 (m, 4H), 2.55−2.45 (m, 1H), 2.44−2.27 (m, 3H), 2.25 (d, J = 7.2 Hz, 2H), 2.16−1.96 (m, 3H), 1.77−1.67 (m, 2H), 1.61−1.43 (m, 4H), 1.22−1.12 (m, 2H). ^{13}C NMR (126 MHz, $CDCl_3$) δ 157.87, 146.72, 139.60, 137.98, 137.26, 133.50, 132.63, 132.30, 131.03, 129.03, 126.06, 122.11, 64.50, 55.36, 55.30, 37.60, 31.96, 31.77, 31.52, 31.09, 30.85, 25.30, one aromatic signal overlapping or not visible. HRMS: $C_{25}H_{30}ClN_2$ $(M + H)^+$ calcd: 393.2092, found: 393.2091. LC−MS: t_R = 3.2 min, purity >98% (254 nm), m/z: 393.2 $(M + H)^+$.

DOI: 10.1021/acs.jmedchem.9b00447
J. Med. Chem. 2019, 62, 6630−6644

*8-Chloro-11-(1-(2-ethylbutyl)piperidin-4-ylidene)-6,11-dihydro-5H-benzo[5,6]cyclohepta[1,2-b]pyridine (**15**).* A mixture of 2-ethylbutanal (85 mg, 0.84 mmol), desloratadine (218 mg, 0.70 mmol), and $NaBH(OAc)_3$ (238 mg, 1.12 mmol) in DCE (10 mL) was stirred at room temperature for 12 h. The resulting solution was diluted with water and extracted with DCM. The organic phase was washed with satd. aq $NaHCO_3$ solution. The organic layer was dried over Na_2SO_4, filtered, and concentrated under vacuum. The crude mixture was purified by column chromatography (cyclohexane/EtOAc/TEA = 40/58/2, v/v/v) to yield the title compound as a pink foam (186 mg, 67% yield).

^{1}H NMR (500 MHz, $CDCl_3$) δ 8.39 (dd, J = 4.9, 1.7 Hz, 1H), 7.42 (dd, J = 7.7, 1.6 Hz, 1H), 7.16−7.11 (m, 3H), 7.08 (dd, J = 7.7, 4.8 Hz, 1H), 3.46−3.29 (m, 2H), 2.88−2.69 (m, 4H), 2.61−2.03 (br m, 8H), 1.49−1.24 (m, 5H), 0.84 (t, J = 7.4 Hz, 6H). ^{13}C NMR (126 MHz, $CDCl_3$) δ 157.95, 146.74, 139.83, 139.63, 138.06, 137.25, 133.51, 132.64, 132.27, 131.04, 129.04, 126.06, 122.10, 62.44, 55.60, 55.52, 38.06, 31.99, 31.56, 31.15, 30.92, 24.33, 10.99. HRMS: $C_{25}H_{32}ClN_2$ $(M + H)^+$ calcd: 395.2249, found: 395.2244. LC−MS: t_R = 3.3 min, purity >98% (254 nm), m/z: 395.2 $(M + H)^+$.

*8-Chloro-11-(1-(cyclobutylmethyl)piperidin-4-ylidene)-6,11-dihydro-5H-benzo[5,6]cyclohepta[1,2-b]pyridine (**16**).* A mixture of (bromomethyl)cyclobutane (208 mg, 1.40 mmol), desloratadine (218 mg, 0.70 mmol), and 60% NaH dispersion (41.6 mg, 1.05 mmol) in DMF (10 mL) was stirred at room temperature for 10 h. The resulting solution was diluted with water and extracted with DCM. The organic phase was washed with satd. aq $NaHCO_3$ solution. The organic layer was dried over Na_2SO_4, filtered, and concentrated under vacuum. The crude mixture was purified by column chromatography (cyclohexane/EtOAc/TEA = 40/58/2, v/v/v) to yield the title compound as a pink foam (150 mg, 56% yield).

^{1}H NMR (500 MHz, $CDCl_3$) δ 8.38 (d, J = 4.9, 1.4 Hz, 1H), 7.41 (d, J = 7.6 Hz, 1H), 7.15−7.08 (m, 3H), 7.06 (dd, J = 7.7, 4.8 Hz, 1H), 3.44−3.30 (m, 2H), 2.85−2.73 (m, 2H), 2.74−2.66 (m, 2H), 2.56−2.44 (m, 2H), 2.43−2.25 (m, 5H), 2.12−1.96 (m, 4H), 1.92−1.80 (m, 1H), 1.79−1.70 (m, 1H), 1.69−1.58 (m, 2H). ^{13}C NMR (126 MHz, $CDCl_3$) δ 157.78, 146.73, 139.60, 139.24, 137.93, 137.29, 133.49, 132.66, 132.46, 130.99, 129.03, 126.07, 122.13, 65.28, 55.13, 55.07, 34.36, 31.94, 31.53, 31.05, 30.80, 28.32, 18.93. HRMS: $C_{24}H_{28}ClN_2$ $(M + H)^+$ calcd: 379.1936, found: 379.1923. LC−MS: t_R = 3.1 min, purity >96% (254 nm), m/z: 379.2 $(M + H)^+$.

*8-Chloro-11-(1-(cyclopropylmethyl)piperidin-4-ylidene)-6,11-dihydro-5H-benzo[5,6]cyclohepta[1,2-b]pyridine (**17**).* A mixture of cyclopropanecarboxaldehyde (59 mg, 0.84 mmol), desloratadine (218 mg, 0.70 mmol), and $NaBH(OAc)_3$ (238 mg, 1.12 mmol) in DCE (10 mL) was stirred at room temperature for 12 h. The resulting solution was diluted with water and extracted with DCM. The organic phase was washed with satd. aq $NaHCO_3$ solution. The organic layer was dried over Na_2SO_4, filtered, and concentrated under vacuum. The crude mixture was purified by column chromatography (cyclohexane/EtOAc/TEA = 40/58/2, v/v/v) to yield the title compound as a pink foam (132 mg, 52% yield).

^{1}H NMR (500 MHz, $CDCl_3$) δ 8.39 (dd, J = 4.8, 1.6 Hz, 1H), 7.42 (dd, J = 7.7, 1.6 Hz, 1H), 7.16−7.09 (m, 3H), 7.07 (dd, J = 7.6, 4.7 Hz, 1H), 3.44−3.30 (m, 2H), 2.93−2.73 (m, 4H), 2.59−2.50 (m, 1H), 2.48−2.31 (m, 3H), 2.24 (d, J = 6.5 Hz, 2H), 2.21−2.12 (m, 2H), 0.92−0.79 (m, 1H), 0.53−0.43 (m, 2H), 0.06 (app q, 2H). ^{13}C NMR (126 MHz, $CDCl_3$) δ 157.78, 146.76, 139.61, 139.24, 137.94, 137.32, 133.51, 132.70, 132.58, 131.01, 129.05, 126.10, 122.17, 63.74, 55.10, 55.05, 31.96, 31.55, 31.05, 30.80, 8.52, 4.11, 4.09. HRMS: $C_{23}H_{26}ClN_2$ $(M + H)^+$ calcd: 365.1779, found: 365.1773. LC−MS: t_R = 2.9 min, purity >99% (254 nm), m/z: 365.1 $(M + H)^+$.

*8-Chloro-11-(1-cyclohexylpiperidin-4-ylidene)-6,11-dihydro-5H-benzo[5,6]cyclohepta[1,2-b]pyridine (**18**).* A mixture of cyclohexanone (82 mg, 0.84 mmol), desloratadine (218 mg, 0.70 mmol), and $NaBH(OAc)_3$ (238 mg, 1.12 mmol) in DCE (10 mL) was stirred at room temperature for 12 h. The resulting solution was diluted with water and extracted with DCM. The organic phase was washed with satd. aq $NaHCO_3$ solution. The organic layer was dried over Na_2SO_4, filtered, and concentrated under vacuum. The crude mixture was purified by column chromatography (cyclohexane/EtOAc/TEA = 40/58/2, v/v/v) to yield the title compound as a pink foam (192 mg, 70% yield).

^{1}H NMR (500 MHz, $CDCl_3$) δ 8.39 (dd, J = 4.8, 1.5 Hz, 1H), 7.42 (d, J = 7.6, 1H), 7.16−7.09 (m, 3H), 7.06 (dd, J = 7.7, 4.8 Hz, 1H), 3.44−3.30 (m, 2H), 2.86−2.71 (m, 4H), 2.53−2.44 (m, 1H), 2.44−2.23 (m, 6H), 1.88−1.69 (m, 4H), 1.60 (app d, J = 13.6 Hz, 1H), 1.27−1.12 (m, 4H), 1.12−1.00 (m, 1H). ^{13}C NMR (126 MHz, $CDCl_3$) δ 157.92, 146.74, 139.86, 139.60, 137.96, 137.25, 133.52, 132.64, 132.24, 131.10, 129.05, 126.06, 122.12, 63.76, 50.71, 50.59, 32.00, 31.64, 31.54, 31.38, 29.05, 28.91, 26.47, 26.17. HRMS: $C_{25}H_{30}ClN_2$ $(M + H)^+$ calcd: 393.2092, found: 393.2083. LC−MS: t_R = 3.1 min, purity >99% (254 nm), m/z: 393.2 $(M + H)^+$.

*8-Chloro-11-(1-cyclopentylpiperidin-4-ylidene)-6,11-dihydro-5H-benzo[5,6]cyclohepta[1,2-b]pyridine (**19**).* A mixture of cyclopentanone (70 mg, 0.84 mmol), desloratadine (218 mg, 0.70 mmol), and $NaBH(OAc)_3$ (238 mg, 1.12 mmol) in DCE (10 mL) was stirred at room temperature for 12 h. The resulting solution was diluted with water and extracted with DCM. The organic phase was washed with satd. aq $NaHCO_3$ solution. The organic layer was dried over Na_2SO_4, filtered, and concentrated under vacuum. The crude mixture was purified by column chromatography (cyclohexane/EtOAc/TEA = 40/58/2, v/v/v) to yield the title compound as a pink foam (189 mg, 71% yield).

^{1}H NMR (500 MHz, $CDCl_3$) δ 8.38 (d, J = 4.8, 1H), 7.41 (d, J = 7.6 Hz, 1H), 7.15−7.08 (m, 3H), 7.06 (dd, J = 7.7, 4.8 Hz, 1H), 3.44−3.29 (m, 2H), 2.87−2.72 (m, 4H), 2.57−2.39 (m, 3H), 2.38−2.29 (m, 2H), 2.19−2.07 (m, 2H), 1.87−1.74 (m, 2H), 1.70−1.59 (m, 2H), 1.55−1.45 (m, 2H), 1.45−1.33 (m, 2H). ^{13}C NMR (126 MHz, $CDCl_3$) δ 157.81, 146.73, 139.59, 139.45, 137.87, 137.26, 133.52, 132.66, 132.27, 131.05, 129.04, 126.07, 122.13, 67.41, 54.13, 54.10, 31.98, 31.53, 31.13, 30.85, 30.70, 24.34. HRMS: $C_{24}H_{28}ClN_2$ $(M + H)^+$ calcd: 379.1936, found: 379.1921. LC−MS: t_R = 3.0 min, purity >99% (254 nm), m/z: 379.1 $(M + H)^+$.

*8-Chloro-11-(1-cyclobutylpiperidin-4-ylidene)-6,11-dihydro-5H-benzo[5,6]cyclohepta[1,2-b]pyridine (**20**).* A mixture of cyclobutanone (59 mg, 0.84 mmol), desloratadine (218 mg, 0.70 mmol), and $NaBH(OAc)_3$ (238 mg, 1.12 mmol) in DCE (10 mL) was stirred at room temperature for 12 h. The resulting solution was diluted with water and extracted with DCM. The organic phase was washed with satd. aq $NaHCO_3$ solution. The organic layer was dried over Na_2SO_4, filtered, and concentrated under vacuum. The crude mixture was purified by column chromatography (cyclohexane/EtOAc/TEA = 40/58/2, v/v/v) to yield the title compound as a pink foam (145 mg, 57% yield).

^{1}H NMR (500 MHz, $CDCl_3$) δ 8.39 (d, J = 4.6 Hz, 1H), 7.42 (d, J = 7.6 Hz, 1H), 7.15−7.09 (m, 3H), 7.09−7.05 (m, 1H), 3.45−3.30 (m, 2H), 2.87−2.74 (m, 2H), 2.74−2.60 (m, 3H), 2.55−2.46 (m, 1H), 2.46−2.28 (m, 3H), 2.05−1.86 (m, 6H), 1.74−1.57 (m, 2H). ^{13}C NMR (126 MHz, $CDCl_3$) δ 157.78, 146.77, 139.60, 139.01, 137.89, 137.33, 133.53, 132.78, 132.74, 130.99, 129.09, 126.12, 122.21, 60.32, 51.24, 51.23, 31.97, 31.53, 30.65, 30.38, 27.42, 14.35. HRMS: $C_{23}H_{26}ClN_2$ $(M + H)^+$ calcd: 365.1779, found: 365.1772. LC−MS: t_R = 2.9 min, purity >99% (254 nm), m/z: 365.2 $(M + H)^+$.

*8-Chloro-11-(1-cyclopropylpiperidin-4-ylidene)-6,11-dihydro-5H-benzo[5,6]cyclohepta[1,2-b]pyridine (**21**).* A mixture of (1-ethoxycyclopropoxy)trimethylsilane (347 mg, 2.00 mmol), desloratadine (622 mg, 2.00 mmol), AcOH (111 mg, 2.00 mmol), and sodium triacetoxyborohydride (604 mg, 3.20 mmol) in DCM (10 mL) was stirred at room temperature for 48 h. The resulting solution was diluted with water and extracted with DCM. The organic phase was washed with satd. aq $NaHCO_3$ solution. The organic layer was dried over Na_2SO_4, filtered, and concentrated under vacuum. The crude mixture was purified by reverse-phase column chromatography (H_2O/MeCN/HCOOH). The product fraction was evaporated, extracted with DCM/satd. aq Na_2CO_3 solution, dried ($MgSO_4$), and concentrated to yield the title compound as a pink foam (124 mg, 17% yield).

^{1}H NMR (500 MHz, $CDCl_3$) δ 8.39 (dd, J = 4.9, 1.5 Hz, 1H), 7.43 (dd, J = 7.8, 1.6 Hz, 1H), 7.16−7.10 (m, 3H), 7.08 (dd, J = 7.7, 4.7

DOI: 10.1021/acs.jmedchem.9b00447
J. Med. Chem. 2019, 62, 6630−6644

Hz, 1H), 3.45−3.32 (m, 2H), 2.92−2.74 (m, 4H), 2.50−2.42 (m, 1H), 2.40−2.26 (m, 5H), 1.60−1.50 (m, 1H), 0.47−0.35 (m, 4H). ^{13}C NMR (126 MHz, $CDCl_3$) δ 157.85, 146.75, 139.58, 139.35, 137.95, 137.30, 133.51, 132.69, 132.66, 131.01, 129.08, 126.10, 122.17, 55.16, 38.39, 31.97, 31.52, 31.00, 30.74, 6.09, one aliphatic signal overlapping or not visible. HRMS: $C_{22}H_{24}ClN_2$ $(M + H)^+$ calcd: 351.1623, found: 351.1610. LC−MS: t_R = 2.9 min, purity >98% (254 nm), m/z: 351.2 $(M + H)^+$.

*8-Chloro-11-(1-isopropylpiperidin-4-ylidene)-6,11-dihydro-5H-benzo[5,6]cyclohepta[1,2-b]pyridine (**22**).* A mixture of propan-2-one (49 mg, 0.84 mmol), desloratadine (218 mg, 0.70 mmol), and $NaBH(OAc)_3$ (238 mg, 1.12 mmol) in DCE (10 mL) was stirred at room temperature for 12 h. The resulting solution was diluted with water and extracted with DCM. The organic phase was washed with satd. aq $NaHCO_3$ solution. The organic layer was dried over Na_2SO_4, filtered, and concentrated under vacuum. The crude mixture was purified by column chromatography (cyclohexane/EtOAc/TEA = 40/58/2, v/v/v) to yield the title compound as a pink foam (101 mg, 41% yield).

^{1}H NMR (500 MHz, $CDCl_3$) δ 8.39 (dd, J = 4.8, 1.7 Hz, 1H), 7.43 (dd, J = 7.7, 1.7 Hz, 1H), 7.16−7.10 (m, 3H), 7.08 (dd, J = 7.6, 4.8 Hz, 1H), 3.45−3.32 (m, 2H), 2.87−2.69 (m, 5H), 2.55−2.47 (m, 1H), 2.46−2.22 (m, 5H), 1.04 (d, J = 6.6 Hz, 3H), 1.03 (d, J = 6.6 Hz, 3H). ^{13}C NMR (126 MHz, $CDCl_3$) δ 157.87, 146.76, 139.62, 137.93, 137.30, 133.55, 132.70, 132.43, 131.08, 129.08, 126.10, 122.17, 54.57, 50.34, 50.19, 32.01, 31.56, 31.40, 31.13, 18.60, 18.45, one aromatic signal overlapping or not visible. HRMS: $C_{22}H_{26}ClN_2$ $(M + H)^+$ calcd: 353.1779, found: 353.1770. LC−MS: t_R = 2.9 min, purity >95% (254 nm), m/z: 353.2 $(M + H)^+$.

*8-Chloro-11-(1-ethylpiperidin-4-ylidene)-6,11-dihydro-5H-benzo[5,6]cyclohepta[1,2-b]pyridine (**23**).* A mixture of acetaldehyde (37 mg, 0.84 mmol), desloratadine (218 mg, 0.70 mmol), and $NaBH(OAc)_3$ (238 mg, 1.12 mmol) in DCE (10 mL) was stirred at room temperature for 12 h. The resulting solution was diluted with water and extracted with DCM. The organic phase was washed with satd. aq $NaHCO_3$ solution. The organic layer was dried over Na_2SO_4, filtered, and concentrated under vacuum. The crude mixture was purified by column chromatography (cyclohexane/EtOAc/TEA = 40/58/2, v/v/v) to yield the title compound as a pink foam (65 mg, 27% yield).

^{1}H NMR (300 MHz, $CDCl_3$) δ 8.40 (dd, J = 4.8, 1.6 Hz, 1H), 7.43 (dd, J = 7.7, 1.7 Hz, 1H), 7.19−7.11 (m, 3H), 7.08 (dd, J = 7.7, 4.8 Hz, 1H), 3.48−3.29 (m, 2H), 2.91−2.70 (m, 4H), 2.62−2.50 (m, 1H), 2.50−2.29 (m, 5H), 2.24−2.05 (m, 2H), 1.09 (t, J = 7.2 Hz, 3H). ^{13}C NMR (126 MHz, $CDCl_3$) δ 157.76, 146.78, 139.64, 139.14, 137.93, 137.36, 133.54, 132.75, 132.66, 131.01, 129.08, 126.13, 122.21, 54.65, 54.59, 52.31, 31.97, 31.57, 31.05, 30.79, 12.23. HRMS: $C_{21}H_{24}ClN_2$ $(M + H)^+$ calcd: 339.1623, found: 339.1608. LC−MS: t_R = 2.7 min, purity >97% (254 nm), m/z: 339.1 $(M + H)^+$.

*8-Chloro-11-(1-methylpiperidin-4-ylidene)-6,11-dihydro-5H-benzo[5,6]cyclohepta[1,2-b]pyridine fumarate (**24**).* To a solution of desloratadine (5.00 g, 16.1 mmol) in DCM (150 mL) were added MeOH (75 mL), aq formaldehyde solution (ca. 13.4 M, 2.40 mL, 32.2 mmol) and AcOH (1.29 mL, 22.5 mmol), and the resulting mixture was stirred at room temperature for 15 min. Subsequently, $NaBH(OAc)_3$ (5.11 g, 24.1 mmol) was added and the resulting mixture was stirred for 1.5 h at room temperature. The reaction mixture was diluted with 1 M aqueous NaOH (600 mL) and extracted with DCM (2 × 200 mL). The combined organic phases were washed with brine (200 mL), dried over Na_2SO_4, filtered, and concentrated in vacuo. Purification by flash column chromatography (DCM/MeOH/TEA 190:5:5) gave the free base (3.96 g), which was subsequently converted to the fumaric acid salt to obtain the title compound as a white solid (4.27 g, 60%).

^{1}H NMR (500 MHz, DMSO-d_6) δ 8.36−8.32 (m, 1H), 7.57 (d, J = 7.6 Hz, 1H), 7.31 (d, J = 2.0 Hz, 1H), 7.24−7.17 (m, 2H), 7.09 (d, J = 8.2 Hz, 1H), 6.55 (s, 2H), 3.37−3.24 (m, 2H), 2.89−2.77 (m, 4H), 2.48−2.38 (m, 4H), 2.36 (s, 3H), 2.31−2.22 (m, 2H). ^{13}C NMR (126 MHz, DMSO-d_6) δ 167.0, 156.7, 146.4, 140.2, 137.8, 137.5, 135.3, 134.6, 133.3, 133.2, 131.6, 130.7, 129.0, 125.7, 122.4, 55.1, 44.2, 30.9, 30.6, 29.2, 29.1. HRMS: $C_{20}H_{22}ClN_2$ $(M + H)^+$ calcd: 325.1466, found 325.1452. LC−MS: t_R = 2.9 min, purity >99% (254 nm), m/z: 324.9 $(M + H)^+$.

*(4-Chlorophenyl)(4-iodophenyl)methanol (**25**).* (4-Chlorophenyl)magnesium bromide (1.0 M in Et_2O) (3.23 mL, 3.23 mmol) was added dropwise over 15 min to a stirred solution of 4-iodobenzaldehyde (500 mg, 2.16 mmol) in Et_2O (4 mL) at 0 °C under nitrogen. The mixture was allowed to warm to room temperature and stirred for a further 16 h. Satd. aq NH_4Cl (1 mL) was added carefully (CAUTION! Exotherm and vigorous bubbling). After bubbling had ceased, the mixture was partitioned between Et_2O (10 mL) and satd. aq NH_4Cl (5 mL). The organic phase was washed with brine (5 mL), dried ($MgSO_4$), filtered, and evaporated to give the title compound (655 mg, 88%) as a cream solid.

^{1}H NMR (400 MHz, $CDCl_3$) δ 7.59 (d, J = 8.62 Hz, 2H), 7.27−7.13 (m, 4H), 7.02 (d, J = 8.36 Hz, 2H), 5.68 (s, 1H).

*1-Chloro-4-(chloro(4-iodophenyl)methyl)benzene (**26**).* $SOCl_2$ (0.138 mL, 1.89 mmol) was added dropwise to a stirred solution of **25** (0.65 g, 1.89 mmol) in DCM (9.29 mL) at room temperature. After 20 h, the solvent was evaporated under vacuum to give the product (0.653 g, 1.799 mmol, 95%) as a purple solid.

^{1}H NMR (400 MHz, $CDCl_3$) δ 7.63−7.58 (m, 2H), 7.27−7.16 (m, 4H), 7.07−7.02 (m, 2H), 5.94 (s, 1H).

*2-(4-((4-Chlorophenyl)(4-iodophenyl)methyl)piperazin-1-yl)-ethanol (**27**).* A solution of 2-(piperazin-1-yl)ethanol (0.206 g, 1.58 mmol) in toluene (1 mL) was added to **26** (0.637 g, 1.75 mmol) and the mixture was stirred at 80 °C under nitrogen for 20 h. The mixture was diluted with DCM and purified by ion-exchange chromatography (strong cation exchange) eluting with 1 M NH_3/MeOH. Fractions containing product were purified by flash silica chromatography (elution gradient 0−5% MeOH−NH_3 (3.5 M) in DCM) to afford the product (165 mg, 0.361 mmol, 21%) as a white solid.

^{1}H NMR (600 MHz, DMSO-d_6) 7.65 (d, J = 8.1 Hz, 2H), 7.39 (d, J = 8.4 Hz, 2H), 7.34 (d, J = 8.4 Hz, 2H), 7.20 (d, J = 8.2 Hz, 2H), 4.15 (s, 1H), 4.32 (s, 1H), 3.5−3.42 (m, 2H), 2.48−2.41 (m, 4H), 2.38 (t, J = 6.0 Hz, 2H), 2.33−2.24 (m, 4H). LC−MS (ESI) m/z 457.

*(S)-2-(2-(4-((4-Chlorophenyl)(4-iodophenyl)methyl)piperazin-1-yl)ethoxy)acetic Acid (**28**).* KOH (79 mg, 1.41 mmol) was added to a stirred solution of **27** (161 mg, 0.35 mmol) in DMF (641 μL) at 0 °C and the mixture was stirred for 90 min. Sodium 2-chloroacetate (82 mg, 0.70 mmol) was added and the mixture was stirred for 3 h. Water (3 mL) was added and the pH was adjusted to 9−10 with aq HCl (1 M). The mixture was washed with EtOAc (2 × 1 mL) and the pH was adjusted to 4−5 with aq HCl (1 M). The mixture was extracted with DCM (3 × 2 mL). The combined DCM phases were washed with brine (2 mL), dried ($MgSO_4$), filtered, and evaporated to give, after trituration with Et_2O, racemic product (103 mg, 0.200 mmol, 57%) as an off-white solid.

^{1}H NMR (600 MHz, DMSO-d_6) 7.69−7.65 (m, 2H), 7.44−7.4 (m, 2H), 7.38−7.34 (m, 2H), 7.22 (d, J = 8.4 Hz, 2H), 3.87 (s, 2H), 4.39 (s, 1H), 3.62 (t, J = 5.5 Hz, 2H), 2.85−2.63 (m, 6H), 2.46−2.27 (m, 4H). LC−MS (ESI) m/z 515.

The stereoisomers were separated by chromatography using a Chiralpak OD column, 5 μm silica, 20 mm diameter, 250 mm length, eluting with 95/05/0.2/0.1 mixture of MeCN/MeOH/AcOH/TEA to give the desired isomer (first eluted) (*S*)-2-(2-(4-((4-chlorophenyl)(4-iodophenyl)methyl)piperazin-1-yl)ethoxy)acetic acid (*S*)-**28** (7.8 mg)

(R)-5-(4-((4-Chlorophenyl)([4-^{3}H]phenyl)methyl)piperazin-1-yl)-pentanoic Acid ([^{3}H]Levocetirizine). Precursor (*S*)-**28** (0.8 mg, 1.55 μmol), Pd (10% on carbon, 0.5 mg, 0.47 μmol), and Et_3N (5 μL, 0.04 mmol) were mixed in EtOH (200 μL). The flask was fitted to the tritium manifold. The mixture was freeze−pump−thaw degassed and was then stirred under tritium gas (63.5 GBq) at 162 mbar for 2.5 h. The reaction mixture was filtered through a poly(tetrafluoroethylene) filter (Whatman 0.45 μm) and washed thoroughly with more EtOH (5 mL). The solution was lyophilized to remove labile tritium, more EtOH (5 mL) was addeAmyloid Inhbitorsd, and the mixture was again lyophilized. Purification by preparative HPLC (Waters XBridge C18 column, 5 μm, 4.6 × 150 mm^2) using decreasingly polar mixtures

DOI: 10.1021/acs.jmedchem.9b00447
J. Med. Chem. 2019, 62, 6630−6644

of water (containing 0.1% TFA) and MeCN as eluents followed by further preparative HPLC (Waters XBridge C18 column, 5 μm, 4.6 × 150 mm^2), using decreasingly polar mixtures of water (containing 0.1% ammonia) and MeCN as eluents, afforded [^{3}H]levocetirizine (728 MBq), which was dissolved in EtOH (10 mL) for storage as a colorless solution.

Radiochemical purity >98% by HPLC. Chiral purity 93% enantiomeric excess by HPLC (obtained on ethyl ester derivative by standing in ethanol with TFA for 3 days). LC−MS (ESI) m/z 391 $[M + H]^+$. ^{1}H NMR (640 MHz, DMSO-d_6) 7.20 (t, J = 7.8). Specific activity by mass spectrometry: 956 GBq mmol^{-1}.

■ ASSOCIATED CONTENT

Supporting Information

The Supporting Information is available free of charge on the ACS Publications website at DOI: 10.1021/acs.jmedchem.9b00447.

Characterization of the kinetics of binding and functional inhibition for H_1R antagonists (Table S1); correlations between key physicochemical properties of rupatadine analogues (**1**−**24**) vs the respective pK_i and KRI values at the H_1R (Figure S1); physicochemical properties of **1**−**24** (Table S2); docked binding poses of **1**−**24** in the H_1R binding pocket (Figures S2 and S3); and ^{1}H NMR and ^{13}C NMR spectroscopy data as well as high-resolution mass spectroscopy and LC−MS chromatograms (Figures S4−S69) (PDF)

Molecular formula strings and associated biochemical data of **1**−**24** (CSV)

■ AUTHOR INFORMATION

Corresponding Author

*E-mail: r.leurs@vu.nl.

ORCID

Albert J. Kooistra: 0000-0001-5514-6021
Michael J. Waring: 0000-0002-9110-8783
Chris de Graaf: 0000-0002-1226-2150
Henry F. Vischer: 0000-0002-0184-6337
Maikel Wijtmans: 0000-0001-8955-8016
Rob Leurs: 0000-0003-1354-2848

Present Addresses

[#]Department of Drug Design and Pharmacology, University of Copenhagen, Universitetsparken 2, 2100 Copenhagen, Denmark (A.J.K.).
[▽]Northern Institute for Cancer Research, School of Natural and Environmental Sciences, Newcastle University, Bedson Building, Newcastle upon Tyne NE1 7RU, United Kingdom (M.J.W.).
[○]Sosei Heptares, Steinmetz Building, Granta Park, Great Abington, Cambridge CB21 6DG, United Kingdom (C.d.G.).

Author Contributions

[⊥]R.B. and Z.W. contributed equally to this work.

Notes

The authors declare no competing financial interest.

■ ACKNOWLEDGMENTS

Hans Custers is thanked for technical assistance. This research was financially supported by the EU/EFPIA Innovative Medicines Initiative (IMI) Joint Undertaking, K4DD (grant no. 115366) as well as by the China Scholarship Council (CSC) (grant no. 201506270163).

■ ABBREVIATIONS

DCE, dichloroethane; DCM, dichloromethane; DMF, dimethylformamide; DMSO, dimethylsulfoxide; GPCR, G protein-coupled receptor; H_1R, histamine H_1 receptor; KRI, kinetic rate index; RecT, recovery time; SKR, structure−kinetics relationship; TFA, trifluoroacetic acid; TEA, triethylamine

■ REFERENCES

(1) Swinney, D. C. Biochemical mechanisms of drug action: what does it take for success? *Nat. Rev. Drug Discovery* **2004**, *3*, 801−808.
(2) Swinney, D. C. Biochemical mechanisms of new molecular entities (NMEs) approved by United States FDA during 2001-2004: mechanisms leading to optimal efficacy and safety. *Curr. Top. Med. Chem.* **2006**, *6*, 461−478.
(3) Copeland, R. A.; Pompliano, D. L.; Meek, T. D. Drug-target residence time and its implications for lead optimization. *Nat. Rev. Drug Discovery* **2006**, *5*, 730−739.
(4) Swinney, D. C. Applications of binding kinetics to drug discovery. *Pharm. Med.* **2008**, *22*, 23−34.
(5) Copeland, R. A. The drug−target residence time model: a 10-year retrospective. *Nat. Rev. Drug Discovery* **2016**, *15*, 87−95.
(6) Hoffmann, C.; Castro, M.; Rinken, A.; Leurs, R.; Hill, S. J.; Vischer, H. F. Ligand residence time at G-protein-coupled receptors-why we should take our time to study it. *Mol. Pharmacol.* **2015**, *88*, 552−560.
(7) Guo, D.; Hillger, J. M.; IJzerman, A. P.; Heitman, L. H. Drug-target residence time-a case for G protein-coupled receptors. *Med. Res. Rev.* **2014**, *34*, 856−892.
(8) Lu, H.; Tonge, P. J. Drug-target residence time: critical information for lead optimization. *Curr. Opin. Chem. Biol.* **2010**, *14*, 467−474.
(9) Vauquelin, G.; Charlton, S. J. Long-lasting target binding and rebinding as mechanisms to prolong in vivo drug action. *Br. J. Pharmacol.* **2010**, *161*, 488−508.
(10) Folmer, R. H. A. Drug target residence time: a misleading concept. *Drug Discovery Today* **2018**, *23*, 12−16.
(11) Dahl, G.; Akerud, T. Pharmacokinetics and the drug-target residence time concept. *Drug Discovery Today* **2013**, *18*, 697−707.
(12) de Witte, W. E. A.; Danhof, M.; van der Graaf, P. H.; de Lange, E. C. M. In vivo target residence time and kinetic selectivity: the association rate constant as determinant. *Trends Pharmacol. Sci.* **2016**, *37*, 831−842.
(13) Louizos, C.; Yáñez, J. A.; Forrest, M. L.; Davies, N. M. Understanding the hysteresis loop conundrum in pharmacokinetic/pharmacodynamic relationships. *J. Pharm. Pharm. Sci.* **2014**, *17*, 34−91.
(14) Vauquelin, G. Effects of target binding kinetics on in vivo drug efficacy: k_{off}, k_{on} and rebinding. *Br. J. Pharmacol.* **2016**, *173*, 2319−2334.
(15) de Witte, W. E. A.; Vauquelin, G.; van der Graaf, P. H.; de Lange, E. C. M. The influence of drug distribution and drug-target binding on target occupancy: the rate-limiting step approximation. *Eur. J. Pharm. Sci.* **2017**, *109*, S83−S89.
(16) Santos, R.; Ursu, O.; Gaulton, A.; Bento, A. P.; Donadi, R. S.; Bologa, C. G.; Karlsson, A.; Al-Lazikani, B.; Hersey, A.; Oprea, T. I.; Overington, J. P. A comprehensive map of molecular drug targets. *Nat. Rev. Drug Discovery* **2017**, *16*, 19−34.
(17) Simons, F. E. R.; Simons, K. J. Histamine and H1-antihistamines: celebrating a century of progress. *J. Allergy Clin. Immunol.* **2011**, *128*, 1139−1150.
(18) Schoepke, N.; Church, M.; Maurer, M. The inhibition by levocetirizine and fexofenadine of the histamine-induced wheal and flare response in healthy caucasian and japanese volunteers. *Acta Derm. Venereol.* **2013**, *93*, 286−293.
(19) Gillard, M.; Van Der Perren, C.; Moguilevsky, N.; Massingham, R.; Chatelain, P. Binding characteristics of cetirizine and levocetirizine to human H1 histamine receptors: contribution of Lys191 and Thr194. *Mol. Pharmacol.* **2002**, *61*, 391−399.

DOI: 10.1021/acs.jmedchem.9b00447
J. Med. Chem. 2019, 62, 6630−6644

(20) Church, M. K. Comparative inhibition by bilastine and cetirizine of histamine-induced wheal and flare responses in humans. *Inflammation Res.* **2011**, *60*, 1107−1112.
(21) Church, M. K. Efficacy and tolerability of rupatadine at four times the recommended dose against histamine- and platelet-activating factor-induced flare responses and ex vivo platelet aggregation in healthy males. *Br. J. Dermatol.* **2010**, *163*, 1330−1332.
(22) Sun, C.; Li, Q.; Pan, L.; Liu, B.; Gu, P.; Zhang, J.; Ding, L.; Wu, C. Development of a highly sensitive LC−MS/MS method for simultaneous determination of rupatadine and its two active metabolites in human plasma: application to a clinical pharmacokinetic study. *J. Pharm. Biomed. Anal.* **2015**, *111*, 163−168.
(23) Solans, A.; Izquierdo, I.; Donado, E.; Antonijoan, R.; Peña, J.; Nadal, T.; Carbó, M.-L.; Merlos, M.; Barbanoj, M. Pharmacokinetic and safety profile of rupatadine when coadministered with azithromycin at steady-state levels: a randomized, open-label, two-way, crossover, Phase I study. *Clin. Ther.* **2008**, *30*, 1639−1650.
(24) Anthes, J. C.; Gilchrest, H.; Richard, C.; Eckel, S.; Hesk, D.; West, R. E.; Williams, S. M.; Greenfeder, S.; Billah, M.; Kreutner, W.; Egan, R. E. Biochemical characterization of desloratadine, a potent antagonist of the human histamine H1 receptor. *Eur. J. Pharmacol.* **2002**, *449*, 229−237.
(25) Gillard, M.; Chatelain, P. Changes in pH differently affect the binding properties of histamine H1 receptor antagonists. *Eur. J. Pharmacol.* **2006**, *530*, 205−214.
(26) Bosma, R.; Moritani, R.; Leurs, R.; Vischer, H. F. BRET-based β-arrestin2 recruitment to the histamine H1 receptor for investigating antihistamine binding kinetics. *Pharmacol. Res.* **2016**, *111*, 679−687.
(27) Gillard, M.; Strolin Benedetti, M.; Chatelain, P.; Baltes, E. Histamine H1 receptor occupancy and pharmacodynamics of second generation H1-antihistamines. *Inflammation Res.* **2005**, *54*, 367−369.
(28) Carceller, E.; Merlos, M.; Giral, M.; Balsa, D.; Almansa, C.; Bartroli, J.; Garcia-Rafanell, J.; Forn, J. (3-Pyridylalkyl)-piperidylidene]benzocycloheptapyridine Derivatives as Dual Antagonists of PAF and Histamine. *J. Med. Chem.* **1994**, *37*, 2697−2703.
(29) Guo, D.; van Dorp, E. J. H.; Mulder-Krieger, T.; van Veldhoven, J. P. D.; Brussee, J.; Ijzerman, A. P.; Heitman, L. H. Dual-point competition association assay: a fast and high-throughput kinetic screening method for assessing ligand-receptor binding kinetics. *J. Biomol. Screening* **2013**, *18*, 309−320.
(30) Motulsky, H.; Mahan, L. The kinetics of competitive radioligand binding predicted by the law of mass action. *Mol. Pharmacol.* **1984**, *25*, 1−9.
(31) Bosma, R.; Stoddart, L. A.; Georgi, V.; Bouzo-Lorenzo, M.; Bushby, N.; Inkoom, L.; Waring, M. J.; Briddon, S. J.; Vischer, H. F.; Sheppard, R. J.; Fernández-Montalván, A.; Hill, S. J.; Leurs, R. Probe dependency in the determination of ligand binding kinetics at a prototypical G protein-coupled receptor. *Sci. Rep.* **2019**, *9* (1), 7906.
(32) Piwinski, J. J.; Wong, J. K.; Green, M. J.; Ganguly, A. K.; Billah, M. M.; West, R. E.; Kreutner, W. Dual antagonists of platelet-activating factor and histamine: identification of structural requirements for dual activity of N-acyl-4-(5,6-dihydro-11H-benzo[5,6]-cyclohepta[1,2-b]pyridin-11-ylidene)piperidines. *J. Med. Chem.* **1991**, *34*, 457−461.
(33) Zhong, D.; Blume, H. HPLC-determination of loratadine and its active metabolite descarboethoxyloratadine in human plasma. *Pharmazie* **1994**, *49*, 736−739.
(34) Okada, M.; Hasumi, K.; Nishimoto, T.; Yoshida, M.; Ishitani, K.; Aotsuka, T.; Kanazawa, H. Heterocyclic Compound and H1 Receptor Antagonist. US20130085127, 2013.
(35) Tanoli, S. T.; Ramzan, M.; Hassan, A.; Sadiq, A.; Jan, M. S.; Khan, F. A.; Ullah, F.; Ahmad, H.; Bibi, M.; Mahmood, T.; Rashid, U. Design, synthesis and bioevaluation of tricyclic fused ring system as dual binding site acetylcholinesterase inhibitors. *Bioorg. Chem.* **2019**, *83*, 336−347.
(36) Baumann, K.; Flohr, A.; Jolidon, S.; Knust, H.; Luebbers, T.; Nettekoven, M. Indol-Amide Compounds as Beta-Amyloid Inhibitors. WO2014060386, 2014.
(37) Zhang, M. Q.; Leurs, R.; Timmerman, H. Histamine H1-Receptor Antagonists. In *Burger's Medicinal Chemistry an Drug Discovery*, 5th ed.; Wolff, M. E., Ed.; Vrije Universiteit: Amsterdam, 1997; Vol. *5*.
(38) Saxena, M.; Gaur, S.; Prathipati, P.; Saxena, A. K. Synthesis of some substituted pyrazinopyridoindoles and 3D QSAR studies along with related compounds: piperazines, piperidines, pyrazinoisoquinolines, and diphenhydramine, and its semi-rigid analogs as antihistamines (H1). *Bioorg. Med. Chem.* **2006**, *14*, 8249−8258.
(39) Tautermann, C. S.; Seeliger, D.; Kriegl, J. M. What can we learn from molecular dynamics simulations for GPCR drug design? *Comput. Struct. Biotechnol. J.* **2015**, *13*, 111−121.
(40) Schmidtke, P.; Luque, F. J.; Murray, J. B.; Barril, X. Shielded hydrogen bonds as structural determinants of binding kinetics: application in drug design. *J. Am. Chem. Soc.* **2011**, *133*, 18903−18910.
(41) Bortolato, A.; Deflorian, F.; Weiss, D. R.; Mason, J. S. Decoding the role of water dynamics in ligand-protein unbinding: CRF1R as a test case. *J. Chem. Inf. Model.* **2015**, *55*, 1857−1866.
(42) Kooistra, A. J.; Kuhne, S.; de Esch, I. J. P.; Leurs, R.; de Graaf, C. A structural chemogenomics analysis of aminergic GPCRs: lessons for histamine receptor ligand design. *Br. J. Pharmacol.* **2013**, *170*, 101−126.
(43) Kuhne, S.; Kooistra, A. J.; Bosma, R.; Bortolato, A.; Wijtmans, M.; Vischer, H. F.; Mason, J. S.; de Graaf, C.; de Esch, I. J. P.; Leurs, R. Identification of ligand binding hot spots of the histamine H1 receptor following structure-based fragment optimization. *J. Med. Chem.* **2016**, *59*, 9047−9061.
(44) Mocking, T.; Bosma, R.; Rahman, S. N.; Verweij, E. W. E.; McNaught-Flores, D. A.; Vischer, H. F.; Leurs, R. Molecular Aspects of Histamine Receptors. In *Histamine Receptors. Preclinical and Clinical Aspects.*; Blandina, P., Passani, M. B., Eds.; Humana Press: Cham, Switzerland, 2016; pp 1−49.
(45) Miller, D. C.; Lunn, G.; Jones, P.; Sabnis, Y.; Davies, N. L.; Driscoll, P. Investigation of the effect of molecular properties on the binding kinetics of a ligand to its biological target. *MedChemComm* **2012**, *3*, 449.
(46) Tresadern, G.; Bartolome, J. M.; Macdonald, G. J.; Langlois, X. Molecular properties affecting fast dissociation from the D2 receptor. *Bioorg. Med. Chem.* **2011**, *19*, 2231−2241.
(47) Bosma, R.; Witt, G.; Vaas, L. A. I.; Josimovic, I.; Gribbon, P.; Vischer, H. F.; Gul, S.; Leurs, R. The target residence time of antihistamines determines their antagonism of the G protein-coupled histamine H1 receptor. *Front. Pharmacol.* **2017**, *8*, 667.
(48) Shimamura, T.; Shiroishi, M.; Weyand, S.; Tsujimoto, H.; Winter, G.; Katritch, V.; Abagyan, R.; Cherezov, V.; Liu, W.; Han, G. W.; Kobayashi, T.; Stevens, R. C.; Iwata, S. Structure of the human histamine H1 receptor complex with doxepin. *Nature* **2011**, *475*, 65−70.
(49) Korb, O.; Stützle, T.; Exner, T. E. Empirical scoring functions for advanced Protein-Ligand docking with PLANTS. *J. Chem. Inf. Model.* **2009**, *49*, 84−96.
(50) Church, M. K.; Church, D. S. Pharmacology of antihistamines. *Indian J. Dermatol.* **2013**, *58*, 219−224.
(51) Slack, R. J.; Russell, L. J.; Hall, D. A.; Luttmann, M. A.; Ford, A. J.; Saunders, K. A.; Hodgson, S. T.; Connor, H. E.; Browning, C.; Clark, K. L. Pharmacological characterization of GSK1004723, a novel, long-acting antagonist at histamine H1 and H3 receptors. *Br. J. Pharmacol.* **2011**, *164*, 1627−1641.
(52) Pan, A. C.; Borhani, D. W.; Dror, R. O.; Shaw, D. E. Molecular determinants of drug-receptor binding kinetics. *Drug Discovery Today* **2013**, *18*, 667−673.
(53) Tautermann, C. S.; Kiechle, T.; Seeliger, D.; Diehl, S.; Wex, E.; Banholzer, R.; Gantner, F.; Pieper, M. P.; Casarosa, P. Molecular basis for the long duration of action and kinetic selectivity of tiotropium for the muscarinic M3 receptor. *J. Med. Chem.* **2013**, *56*, 8746−8756.
(54) Dowling, M. R.; Charlton, S. J. Quantifying the association and dissociation rates of unlabelled antagonists at the muscarinic M3 receptor. *Br. J. Pharmacol.* **2006**, *148*, 927−937.

DOI: 10.1021/acs.jmedchem.9b00447
J. Med. Chem. 2019, 62, 6630−6644

(55) Baell, J. B.; Holloway, G. A. New substructure filters for removal of pan assay interference compounds (PAINS) from screening libraries and for their exclusion in bioassays. *J. Med. Chem.* **2010**, *53*, 2719−2740.
(56) Xie, X.-Q. *PAINS-Remover*, 2019. www.cbligand.org/PAINS/ (accessed Mar 10, 2019).
(57) Cheng, Y.-C.; Prusoff, W. H. Relationship between the inhibition constant (KI) and the concentration of inhibitor which causes 50 per cent inhibition (I50) of an enzymatic reaction. *Biochem. Pharmacol.* **1973**, *22*, 3099−3108.
(58) Marcou, G.; Rognan, D. Optimizing fragment and scaffold docking by use of molecular interaction fingerprints. *J. Chem. Inf. Model.* **2007**, *47*, 195−207.

DOI: 10.1021/acs.jmedchem.9b00447
J. Med. Chem. 2019, 62, 6630−6644